Ab initio calculations of H_{c2} in type-II superconductors: Basic formalism and model calculations

Takafumi Kita
Division of Physics, Hokkaido University, Sapporo 060-0810, Japan

Masao Arai
National Institute for Materials Science, Namiki 1-1, Tsukuba, Ibaraki 305-0044, Japan

(Received 12 March 2004; revised manuscript received 13 October 2004; published 29 December 2004)

Detailed Fermi-surface structures are essential to describe the upper critical field H_{c2} in type-II superconductors, as first noticed by and Hohenberg and Werthamer [Phys. Rev. **153**, 493 (1967)] and shown explicitly by Butler for high-purity cubic Niobium [Phys. Rev. Lett. **44**, 1516 (1980)]. We derive an H_{c2} equation for classic type-II superconductors that is applicable to systems with anisotropic Fermi surfaces and/or energy gaps under arbitrary field directions. It can be solved efficiently by using Fermi surfaces from *ab initio* electronic-structure calculations. Thus, it is expected to enhance our quantitative understanding on H_{c2}. Based on the formalism, we calculate H_{c2} curves for Fermi surfaces of a three-dimensional tight-binding model with cubic symmetry, an isotropic gap, and no impurity scatterings. It is found that, as the Fermi surface approaches to the Brillouin zone boundary, the reduced critical field $h*(T/T_c)$, which is normalized by the initial slope at T_c, is enhanced significantly over the curve for the spherical Fermi surface with a marked upward curvature. Thus, the Fermi-surface anisotropy can be a main source of the upward curvature in H_{c2} near T_c.

DOI: 10.1103/PhysRevB.70.224522 PACS number(s): 74.25.Op, 71.18.+y

I. INTRODUCTION

The upper critical field H_{c2} is one of the most fundamental quantities in type-II superconductors. After the pioneering work by Abrikosov[1] based on the Ginzburg-Landau (GL) equations,[2] theoretical efforts have been made for its quantitative description at all temperatures.[3–41] However, we still have a limited success when compared with those for the electronic structures in the normal state.[42] The purpose of the present paper is to provide a theoretical framework that enables us *ab initio* calculations of H_{c2} as accurate as electronic-structure calculations in the normal state.

Necessary ingredients to be included are (i) nonlocal effects effective at low temperatures, (ii) impurity scattering, (iii) Fermi-surface anisotropy, (iv) strong-coupling effects, (v) gap anisotropy, (vi) mixing of higher Landau levels in the spatial dependence of the pair potential, (vii) Landau-level quantization in the quasiparticle energy,[13,32,35–38] and (viii) fluctuations beyond the mean-field theory.[43] We here derive an H_{c2} equation, which is numerically tractable, including all the effects except (vii) and (viii).

An H_{c2} equation considering the effects (i) and (ii) was obtained by Helfand and Werthamer.[6] It was extended by Hohenberg and Werthamer[9] to take the Fermi-surface anisotropy (iii) into account. Equations with the strong-coupling effects (iv) were derived by Eilenberger and Ambegaokar[11] using Matsubara frequencies and by Werthamer and McMillan[12] on the real energy axis, which are equivalent to one another. Schossmann and Schachinger[27] later incorporated Pauli paramagnetism into the strong-coupling equation. Although an equation including (i)–(iv) was presented by Langmann,[33] it is still rather complicated for carrying out an actual numerical computation. On the other hand, Rieck and Scharnberg[30] presented an efficient H_{c2} equation where the effects (i)–(iii) and (vi) were taken into account, and also (v) in the special case of the clean limit. See also the work by Rieck, Scharnberg, and Schopohl[31] where the strong-coupling effects (v) have also been considered. Our study can be regarded as a direct extension of the Rieck-Scharnberg equation[30] to incorporate (i)–(iv), simultaneously. To this end, we adopt a slightly different and (probably) more convenient procedure of using creation and annihilation operators. We will proceed with clarifying the connections with the Rieck-Scharnberg equation as explicitly as possible.

The remarkable success of the simplified Bardeen-Cooper-Schrieffer (BCS) theory[44,45] tells us that detailed electronic structures are rather irrelevant to the properties of classic superconductors at $H=0$. However, this is not the case for the properties of type-II superconductors in finite magnetic fields, especially in the clean limit, as first recognized by Hohenberg and Werthamer.[9] Their effort to include the Fermi-surface anisotropy in the H_{c2} equation was motivated by the fact that the Helfand-Werthamer theory[6] using the spherical Fermi surface shows neither qualitative nor quantitative agreements with experiments on clean type-II superconductors, such as Nb[46–48] and V.[49] Indeed, angular variation in H_{c2} by 10% was observed at low temperatures in high-quality Nb[46,50,51] and V[50,51] with cubic symmetry.[52] Also, the reduced critical field

$$h*(t) \equiv \frac{H_{c2}(t)}{-\,dH_{c2}(t)/dt|_{t=1}} \quad (t \equiv T/T_c), \tag{1}$$

calculated by Helfand and Werthamer,[6] has $h*(0)=0.727$ in the clean limit, whereas a later experiment on high-purity Nb shows $\langle h*(0)\rangle = 1.06$ for the average overfield directions.[51] Hohenberg and Werthamer[9] carried out a perturbation expansion for cubic materials with respect to the nonlocal correction where the Fermi-surface anisotropy enters. They could thereby provide a qualitative understanding of the H_{c2} aniso-

TABLE I. Equation numbers for the relevant analytic expressions to calculate H_{c2}. The upper critical field H_{c2} corresponds to the point where the smallest eigenvalue of the Hermitian matrix $\mathcal{A}=(\mathcal{A}_{NN'})$ takes zero.

$\langle\cdots\rangle$	$\phi(\mathbf{k}_F)$	B	Φ_0	T_c	l_c	$\overline{v_{F+}}$	$c_{1,2}$	χ_{ij}	$\tilde{\varepsilon}'_n$	$\overline{\beta}$	$\mathcal{A}_{NN'}$	$\mathcal{K}_{NN'}$	$\eta(x)$	$H_{c2}(T\lesssim T_c)$	B_1	B_2	R	$w_{\nu,\mu}$
(4)	(5)	(7)	$hc/2e$	(A5)	(15)	(18)	(19)	(20)	(13)	(30)	(36)	(39)	(41)	(22)	(23)	(A9a)	(24)	(A4)

tropy and the enhancement of $\langle h^*(t)\rangle$ observed in Nb. They also derived an expression for $\langle h^*(0)\rangle$ applicable to anisotropic Fermi surfaces. It was later used by Mattheiss[14] to estimate $\langle h^*(0)\rangle=0.989$ for Nb based on his detailed electronic-structure calculation. The strong dependence of $h^*(t)$ in the clean limit on detailed Fermi-surface structures can also be seen clearly in the numerical results from a model calculation by Rieck and Scharnberg,[30] and from the difference $h^*(0)=0.727$ and 0.591 between spherical and cylindrical Fermi surfaces, respectively.[41]

On the other hand, it was shown by Werthamer and McMillan[12] that the strong-coupling effects change $h^*(t)$ by only $\lesssim 2\%$ for the spherical Fermi surface and cannot be the main reason for the enhancement of $h^*(0)$ in Nb.

The most complete calculation, including the effects (i)–(iv), was performed on pure Nb by Butler.[22,23] He solved the strong-coupling equation by Eilenberger and Ambegaokar,[11] taking full account of the Fermi-surface structure and the phonon spectra from his electronic-structure calculations. He could thereby obtain an excellent agreement with experiments by Williamson[50] with $\langle h^*(0)\rangle=0.96$ and by Kerchner *et al.*[53] However, a later experiment by Sauerzopf *et al.*[51] on a high-purity Nb shows a larger value $\langle h^*(0)\rangle=1.06$, thereby suggesting that there may be some factors missing in Butler's calculation.

Theoretical considerations on the effects (v) and (vi) started much later. It was Takanaka,[18] Teichler,[19] and Pohl and Teichler[20] who included gap anisotropy (v) in the H_{c2} equation. They considered the nonlocal effect perturbatively adopting a separable pair potential. Takanaka studied H_{c2} anisotropy observed in uniaxial crystals, whereas Teichler applied his theory to the H_{c2} anisotropy in cubic Nb. This approach by Teichler was extended by Prohammer and Schachinger[28] to anisotropic polycrystals and used by Weber *et al.*[54] to analyze anisotropy effects in Nb.

The mixing of higher Landau levels (vi) was considered by Takanaka and Nagashima[15] in extending the Hohenberg-Werthamer theory for cubic materials[9] to higher orders in the nonlocal correction. It was also taken into account by Takanaka[18] in the above-mentioned work, Youngner and Klemm[24] in their perturbation expansion with respect to the nonlocal corrections; Scharnberg and Klemm[25] in studying H_{c2} for p-wave superconductors, Rieck and Scharnberg[30] for superconductors with nearly cylindrical model Fermi surfaces, and Prohammer and Carbotte[29] for d-wave superconductors. See also a recent work by Miranović, Machida,[39] and Kogan on MgB_2. Although it plays an important role in the presence of gap anisotropy,[25,29] this mixing was not considered by Teichler[19] and Pohl and Teichler.[20]

Now, one may be convinced that calculations including (i)–(vi) are still absent. Especially, many of the theoretical efforts have been focused only on the special case of cubic materials.[9,15,19,20,22,23] For example, a detailed theory is still absent for the large positive (upward) curvature observed in $H_{c2}(T\lesssim T_c)$ of layered superconductors,[55,56] except a qualitative description by Takanaka[18] and Dalrymple and Prober.[57] Based on these observations, we here derive an H_{c2} equation that is numerically tractable for arbitrary crystal structures and field directions by using Fermi surfaces from *ab initio* electronic-structure calculations. This kind of calculations has been performed only for Nb by Butler so far.[22,23] Making such calculations possible for other materials is expected to enhance our quantitative understanding on H_{c2} substantially.

This paper is organized as follows. Section II considers the weak-coupling model with gap anisotropy and s-wave impurity scattering. We derive an H_{c2} equation valid at all temperatures as well as an analytic expression for $H_{c2}(T\lesssim T_c)$ up to second order in $1-T/T_c$. The main analytic results of Sec. II are listed in Table I for an easy reference. Section III extends the H_{c2} equation so as to include p-wave impurity scattering, spin-orbit impurity scattering, and strong electron-phonon interactions. Section IV presents numerical examples for model Fermi surfaces of a three-dimensional tight-binding model with cubic symmetry. Section V summarizes the paper. We use $k_B=1$ throughout.

II. WEAK-COUPLING H_{c2} EQUATION

A. Fermi-surface harmonics and gap anisotropy

We first specify the gap anisotropy in our consideration with respect to the Fermi-surface harmonics. The Fermi-surface harmonics were introduced by Allen[58] as convenient polynomials in solving the Boltzmann and Eliashberg equations. They were later used by Langmann[33] to derive an H_{c2} equation applicable to anisotropic Fermi surfaces and anisotropic pairing interactions. However, the polynomials constructed by Allen based on the Gram-Schmidt orthonormalization are not very convenient for treating the gap anisotropy. We here adopt an alternative construction starting from the pairing interaction $V(\mathbf{k}_F,\mathbf{k}'_F)$ on the Fermi surface,[59] where $\mathbf{k}_F$ denotes the Fermi wave vector. Evidently $V(\mathbf{k}_F,\mathbf{k}'_F)$ is Hermitian $V^*(\mathbf{k}_F,\mathbf{k}'_F)=V(\mathbf{k}'_F,\mathbf{k}_F)$, and invariant under every symmetry operation R of the group G for the relevant crystal as $RV(\mathbf{k}_F,\mathbf{k}'_F)R^{-1}=V(\mathbf{k}_F,\mathbf{k}'_F)$. We hence consider the following eigenvalue problem:

$$\int dS'_F\rho(\mathbf{k}'_F)V(\mathbf{k}_F,\mathbf{k}'_F)\phi_\gamma^{(\Gamma j)}(\mathbf{k}'_F)=V^{(\Gamma j)}\phi_\gamma^{(\Gamma j)}(\mathbf{k}_F). \quad (2)$$

Here dS_F denotes an infinitesimal area on the Fermi surface and $\rho(\mathbf{k}_F)\equiv[(2\pi)^3N(0)|\mathbf{v}_F|]^{-1}$ with $\mathbf{v}_F$ the Fermi velocity and $N(0)$ the density of states per one spin and per unit volume at

the Fermi energy in the normal state. The superscript Γ denotes an irreducible representation of G, j distinguishes different eigenvalues belonging to Γ, and γ specifies an eigenvector in (Γ, j). This eigenvalue problem was also considered by Pokrovskii[60] without specifying the symmetry. The basis functions thereby obtained naturally have all the properties of Fermi-surface harmonics introduced by Allen.[58] Especially, they satisfy the orthonormality and completeness

$$\langle \phi_{\gamma}^{(\Gamma j)*} \phi_{\gamma'}^{(\Gamma' j')} \rangle = \delta_{\Gamma\Gamma'} \delta_{jj'} \delta_{\gamma\gamma'}, \tag{3a}$$

$$\sum_{\Gamma j \gamma} \phi_{\gamma}^{(\Gamma j)}(\mathbf{k}_{\mathrm{F}}) \phi_{\gamma}^{(\Gamma j)*}(\mathbf{k}_{\mathrm{F}}') = \frac{\delta^2(\mathbf{k}_{\mathrm{F}} - \mathbf{k}_{\mathrm{F}}')}{\rho(\mathbf{k}_{\mathrm{F}})}, \tag{3b}$$

where $\langle \cdots \rangle$ denotes the Fermi-surface average

$$\langle A \rangle \equiv \int dS_{\mathrm{F}} \rho(\mathbf{k}_{\mathrm{F}}) A(\mathbf{k}_{\mathrm{F}}). \tag{4}$$

Using Eqs. (2) and (3), we obtain an alternative expression for the dimensionless pairing interaction $\lambda(\mathbf{k}_{\mathrm{F}}, \mathbf{k}_{\mathrm{F}}') \equiv -N(0) V(\mathbf{k}_{\mathrm{F}}, \mathbf{k}_{\mathrm{F}}')$ as

$$\lambda(\mathbf{k}_{\mathrm{F}}, \mathbf{k}_{\mathrm{F}}') = \sum_{\Gamma j \gamma} \lambda^{(\Gamma j)} \phi_{\gamma}^{(\Gamma j)}(\mathbf{k}_{\mathrm{F}}) \phi_{\gamma}^{(\Gamma j)*}(\mathbf{k}_{\mathrm{F}}'). \tag{5}$$

Thus, it is always possible to express a general pairing interaction as a sum of separable interactions. Notice that the above procedure is applicable also to multiband superconductors. Indeed, we only have to extend the integration over $\mathbf{k}_{\mathrm{F}}$ to all the Fermi surfaces.

The Fermi-surface harmonics can be constructed also from the coupling function $\lambda(\mathbf{k}_{\mathrm{F}}, \mathbf{k}_{\mathrm{F}}', \varepsilon_n - \varepsilon_n') - \mu^*(\mathbf{k}_{\mathrm{F}}, \mathbf{k}_{\mathrm{F}}')$ in the strong-coupling Eliashberg theory,[61,62] where $\varepsilon_n \equiv (2n+1)\pi T$ is the Matsubara energy. Indeed, we only have to specify an appropriate bosonic Matsubara energy $\omega_l \equiv 2l\pi T$ and set $V(\mathbf{k}_{\mathrm{F}}, \mathbf{k}_{\mathrm{F}}') \equiv -[\lambda(\mathbf{k}_{\mathrm{F}}, \mathbf{k}_{\mathrm{F}}', \omega_l) - \mu^*(\mathbf{k}_{\mathrm{F}}, \mathbf{k}_{\mathrm{F}}')]/N(0)$ in Eqs. (2) and (3). We thereby obtain an alternative expression for the coupling function as

$$\lambda(\mathbf{k}_{\mathrm{F}}, \mathbf{k}_{\mathrm{F}}', \varepsilon_n - \varepsilon_n') - \mu^*(\mathbf{k}_{\mathrm{F}}, \mathbf{k}_{\mathrm{F}}') = \sum_{\Gamma j \gamma} [\lambda^{(\Gamma j)}(\varepsilon_n - \varepsilon_n') - \mu^{*(\Gamma j)}] \phi_{\gamma}^{(\Gamma j)}(\mathbf{k}_{\mathrm{F}}) \phi_{\gamma}^{(\Gamma j)*}(\mathbf{k}_{\mathrm{F}}'). \tag{6}$$

We expect that this construction does not depend on the choice of ω_l substantially. It is worth noting that *ab initio* calculations of the coupling function are now possible for phonon-mediated superconductors, as performed recently for MgB_2.[63] Hence *ab initio* constructions of the Fermi-surface harmonics by Eq. (2) can be carried out in principle.

From now on we consider the cases where (i) the system has inversion symmetry and (ii) a single $\lambda^{(\Gamma j)}$ is relevant that belongs to an even-parity one-dimensional representation Γ. Indeed, these conditions are met for most superconductors. Hereafter we will drop all the indices as $\phi_{\gamma}^{(\Gamma j)}(\mathbf{k}_{\mathrm{F}}) \to \phi(\mathbf{k}_{\mathrm{F}})$, for example, and choose $\phi(\mathbf{k}_{\mathrm{F}})$ as a real function.

B. Eilenberger equations

Now, let us derive an H_{c2} equation for the second-order transition in the weak-coupling model with s-wave impurity scattering based on the quasiclassical Eilenberger equations.[64–66] The Eilenberger equations are derived from the Gor'kov equations by assuming a constant density of states near the Fermi energy in the normal state and integrating out an irrelevant energy variable.[64–66] Thus, phenomena closely connected with either the energy dependence of the density of states[26] or the discreteness in the quasiparticle energy levels[13,32,35–38] are beyond the scope of the present consideration. We also do not consider Josephson vortices appearing in very anisotropic layered superconductors.[67] Within the limitations, however, the Eilenberger equations provide one of the most convenient starting points for deriving an H_{c2} equation, as seen below. This approach was also adopted by Rieck and Scharnberg[30] and Rieck *et al.*[31]

We take the external magnetic field $\mathbf{H}$ along the z-axis. In the presence of Pauli paramagnetism, the average flux density B in the bulk is connected with H as $H = B - 4\pi\chi_{\mathrm{n}} B$, where χ_{n} is the normal-state spin susceptibility. The fact that χ_{n} is multiplied by B rather than H corresponds to the fact that the spins respond to the true magnetic field in the bulk. It, hence, follows that B is enhanced over H as

$$B = H/(1 - 4\pi\chi_{\mathrm{n}}). \tag{7}$$

The vector potential in the bulk at $H = H_{c2}$ can be written accordingly as

$$\mathbf{A}(\mathbf{r}) = (0, Bx, 0). \tag{8}$$

The field $\mathbf{H}$ is supposed to be along the direction $(\sin\theta\cos\varphi, \sin\theta\sin\varphi, \cos\theta)$ in the crystallographic coordinates (X, Y, Z). The two coordinate systems are connected by the rotation matrix

$$\mathcal{R} \equiv \begin{bmatrix} \cos\theta\cos\varphi & \cos\theta\sin\varphi & -\sin\theta \\ -\sin\varphi & \cos\varphi & 0 \\ \sin\theta\cos\varphi & \sin\theta\sin\varphi & \cos\theta \end{bmatrix}, \tag{9}$$

as $\mathcal{R}\mathbf{H} = (0, 0, H)^{\mathrm{T}}$, where T denotes transpose. We assume that the vortex lattice is uniform along z.

With the gap anisotropy specified by $\phi(\mathbf{k}_{\mathrm{F}})$ and in the presence of Pauli paramagnetism, the Eilenberger equations reads

$$\left(\varepsilon_n - i\mu_{\mathrm{B}} B + \frac{\hbar}{2\tau}\langle g \rangle + \frac{1}{2}\hbar \mathbf{v}_{\mathrm{F}} \cdot \boldsymbol{\partial} \right) f = \left(\phi\Delta + \frac{\hbar}{2\tau}\langle f \rangle \right) g, \tag{10a}$$

$$\Delta(\mathbf{r}) \ln\frac{T_{c0}}{T} = \pi T \sum_{n=-\infty}^{\infty} \left[\frac{\Delta(\mathbf{r})}{|\varepsilon_n|} - \langle \phi(\mathbf{k}_{\mathrm{F}}) f(\varepsilon_n, \mathbf{k}_{\mathrm{F}}, \mathbf{r}) \rangle \right]. \tag{10b}$$

Here μ_{B} is the Bohr magneton, τ is the relaxation time by nonmagnetic impurity scattering in the second-Born approximation, $\Delta(\mathbf{r})$ is the pair potential, and $\boldsymbol{\partial}$ is defined by

$$\boldsymbol{\partial} \equiv \nabla - i\frac{2\pi}{\Phi_0}\mathbf{A}, \tag{11}$$

with $\Phi_0 \equiv hc/2e$ the flux quantum. We will consider positively charged particles following the convention; the case of

electrons can be obtained directly by $\mathbf{A}\rightarrow-\mathbf{A}$, i.e., reversing the magnetic-field direction. The quasiclassical Green's functions f and g are connected by $g=(1-ff^{\dagger})^{1/2}\mathrm{sgn}(\varepsilon_n)$ with $f^{\dagger}(\varepsilon_n,\mathbf{k}_{\mathrm{F}},\mathbf{r})=f^{*}(-\varepsilon_n,\mathbf{k}_{\mathrm{F}},\mathbf{r})$,[68] and T_{c0} denotes the transition temperature in the clean limit $\tau=\infty$.

To obtain B_{c2}, we formally expand the quasiclassical Green's functions up to the first order in Δ as $f=f^{(1)}$ and $g=\mathrm{sgn}(\varepsilon_n)$. Substituting the expressions into Eqs. (10a) and (10b), we obtain the linearized self-consistency equations as

$$\left[\tilde{\varepsilon}_n'+\frac{\mathrm{sgn}(\varepsilon_n)}{2}\hbar\mathbf{v}_{\mathrm{F}}\cdot\boldsymbol{\partial}\right]f^{(1)}=\phi\Delta+\frac{\hbar}{2\tau}\langle f^{(1)}\rangle, \tag{12a}$$

$$\Delta\ln\frac{T_{c0}}{T}=-\pi T\sum_{n=-\infty}^{\infty}\left(\langle\phi f^{(1)}\rangle-\frac{\Delta}{|\varepsilon_n|}\right), \tag{12b}$$

with

$$\tilde{\varepsilon}_n'\equiv\tilde{\varepsilon}_n-i\mu_{\mathrm{B}}B\,\mathrm{sgn}(\varepsilon_n),\quad \tilde{\varepsilon}_n\equiv|\varepsilon_n|+\frac{\hbar}{2\tau}. \tag{13}$$

C. Operators and basis functions

It is useful to transform the gradient operator in Eq. (10a) as

$$\mathbf{v}_{\mathrm{F}}\cdot\boldsymbol{\partial}=(\overline{v_{\mathrm{F}+}^{*}}a-\overline{v_{\mathrm{F}+}}a^{\dagger})/\sqrt{2}l_{\mathrm{c}}. \tag{14}$$

Here l_{c} denotes $1/\sqrt{2}$ times the magnetic length as

$$l_{\mathrm{c}}\equiv\sqrt{\Phi_0/2\pi B}=\sqrt{\hbar c/2eB}. \tag{15}$$

The operators a and $a^{\dagger}$ are defined by

$$\begin{bmatrix}a\\ a^{\dagger}\end{bmatrix}=\frac{l_{\mathrm{c}}}{\sqrt{2}}\begin{bmatrix}c_1 & ic_2\\ -c_1^{*} & ic_2^{*}\end{bmatrix}\begin{bmatrix}\partial_x\\ \partial_y\end{bmatrix}, \tag{16}$$

where the constants c_1 and c_2 are constrained by

$$c_1c_2^{*}+c_1^{*}c_2=2, \tag{17}$$

so that $[a,a^{\dagger}]=1$. Finally, $\overline{v_{\mathrm{F}+}}$ is defined by

$$\overline{v_{\mathrm{F}+}}\equiv c_2v_{\mathrm{F}x}+ic_1v_{\mathrm{F}y}. \tag{18}$$

The constants (c_1,c_2) can be fixed conveniently by requiring that the gradient term in the Ginzburg-Landau equation be expressed in terms of $a^{\dagger}a$ without using aa and $a^{\dagger}a^{\dagger}$, i.e., the pair potential near T_c be described in terms of the lowest Landau level only. As shown in Appendix I, this condition yields

$$c_1=\left(\frac{\chi_{xx}^2}{\chi_{xx}\chi_{yy}-\chi_{xy}^2}\right)^{1/4} \tag{19a}$$

$$c_2=\left(\frac{\chi_{yy}^2}{\chi_{xx}\chi_{yy}-\chi_{xy}^2}\right)^{1/4}\exp\left(i\tan^{-1}\frac{-\chi_{xy}}{\sqrt{\chi_{xx}\chi_{yy}-\chi_{xy}^2}}\right), \tag{19b}$$

where $\chi_{ij}\equiv\chi_{ij}(T_c)$ is defined by

$$\chi_{ij}\equiv\frac{24(\pi T_c)^3}{7\zeta(3)\langle v_{\mathrm{F}}^2\rangle}\sum_{n=0}^{\infty}\frac{1}{\tilde{\varepsilon}_n^3}\left[\langle\phi^2v_{\mathrm{F}i}v_{\mathrm{F}j}\rangle+\frac{\langle\phi\rangle\langle\phi v_{\mathrm{F}i}v_{\mathrm{F}j}\rangle}{2\tau\varepsilon_n}+\frac{\langle\phi\rangle\langle\phi v_{\mathrm{F}i}v_{\mathrm{F}j}\rangle}{2\tau\varepsilon_n}+\frac{\langle\phi\rangle\langle\phi\rangle\langle v_{\mathrm{F}i}v_{\mathrm{F}j}\rangle}{(2\tau\varepsilon_n)^2}\right], \tag{20}$$

with ζ the Riemann zeta function. Note that χ_{ij} is dimensionless, approaching to δ_{ij} as $\tau\rightarrow\infty$ for the spherical Fermi surface. It is a direct generalization of the χ function introduced by Gor'kov[69] to anisotropic systems.

The operators in Eq. (16) extend (a_-,a_+) introduced by Helfand and Werthamer[6] for anisotropic crystals. For uniaxial crystals, they reduce to the operators used by Takanaka.[18]

Using Eq. (16), we can also make up a set of basis functions to describe vortex-lattice structures as[70]

$$\begin{aligned}\psi_{N\mathbf{q}}(\mathbf{r})=&\sqrt{\frac{2\pi l_{\mathrm{c}}}{c_1a_2\sqrt{\pi}V}}\sum_{n=-\mathcal{N}_{\mathrm{f}}/2+1}^{\mathcal{N}_{\mathrm{f}}/2}\exp\left[iq_y\left(y+\frac{l_{\mathrm{c}}^2q_x}{2}\right)\right]\\&\times\exp\left[i\frac{na_{1x}}{l_{\mathrm{c}}^2}\left(y+l_{\mathrm{c}}^2q_x-\frac{na_{1y}}{2}\right)\right]\\&\times\exp\left[-\frac{c_1c_2}{2}\left(\frac{x-l_{\mathrm{c}}^2q_y-na_{1x}}{c_1l_{\mathrm{c}}}\right)^2\right]\\&\times\frac{1}{\sqrt{2^NN!}}H_N\left(\frac{x-l_{\mathrm{c}}^2q_y-na_{1x}}{c_1l_{\mathrm{c}}}\right).\end{aligned} \tag{21}$$

Here $N=0,1,2,\cdots$ denotes the Landau level, $\mathbf{q}$ is an arbitrary chosen magnetic Bloch vector characterizing the broken translational symmetry of the vortex lattice and specifying the core locations, and V is the volume of the system. The quantities a_{1x} and a_2 are the components of the basic vectors $\mathbf{a}_1$ and $\mathbf{a}_2$ in the xy plane, respectively, with $\mathbf{a}_2\|\hat{\mathbf{y}}$ and $a_{1x}a_2=2\pi l_{\mathrm{c}}^2$, $\mathcal{N}_{\mathrm{f}}^2$ denotes the number of the flux quantum in the system, and $H_N(x)\equiv e^{x^2}(-d/dx)^Ne^{-x^2}$ is the Hermite polynomial. The basis functions are both orthonormal and complete, satisfying $a\psi_{N\mathbf{q}}=\sqrt{N}\psi_{N-1\mathbf{q}}$ and $a^{\dagger}\psi_{N\mathbf{q}}=\sqrt{N+1}\psi_{N+1\mathbf{q}}$.

The function (21) is a direct generalization of the Eilenberger function[10] $\psi_N(\mathbf{r}|\mathbf{r}_0)$ with $c_1=c_2=1$ to anisotropic Fermi surfaces and energy gaps. For $\mathbf{q}=0$ in the clean limit, Eq. (21) reduces to the function obtained by Rieck and Scharnberg[30,71] and Rieck*et al.*,[31] However, they derived it without recourse to the creation and annihilation operators of Eq. (16). These operators have simplified the derivation of the basis functions and will also make the whole calculations below much easier and transparent.

D. Analytic expression of H_{c2} near T_c

Using Eq. (16), it is also possible to obtain an analytic expression for $B_{c2}\equiv H_{c2}/(1-4\pi\chi_{\mathrm{n}})$ near T_c. Let us express it as

$$B_{c2}=B_1(1-t)+B_2(1-t)^2, \tag{22}$$

with $t\equiv T/T_c$. The coefficients B_1 and B_2 determine the initial slope and the curvature, respectively.

It is shown in Appendix I that B_1 is obtained as

$$B_1 \equiv \frac{24\pi R\Phi_0}{7\zeta(3)(\chi_{xx}\chi_{yy}-\chi_{xy}^2)^{1/2}(\hbar\langle v_{\rm F}^2\rangle^{1/2}/T_c)^2}, \tag{23}$$

where ζ is the Riemann zeta function, χ_{ij} is given by Eq. (20), and R is defined by

$$R = 1-\hbar\frac{1-\langle\phi\rangle^2}{2\tau}2\pi T_c\sum_{n=0}^{\infty}\frac{1}{\tilde{\varepsilon}_n^2}. \tag{24}$$

The factor $\hbar\langle v_{\rm F}^2\rangle^{1/2}/T_c$ in the denominator of Eq. (23) is essentially the BCS coherence length.[44] Also, R is dimensionless and approaches unity for $\tau\to\infty$. Equation (23) is a direct generalization of the result by Rieck and Scharnberg[30] for $\phi(\mathbf{k}_{\rm F})=1$ to the cases with gap anisotropy and for arbitrary strength of the impurity scattering.

It is convenient to express $\langle v_{{\rm F}i}v_{{\rm F}j}\rangle$ in Eq. (20) with respect to the crystallographic coordinates (X,Y,Z) to see the anisotropy in B_1 manifestly. Using Eq. (9), $v_{{\rm F}x}$ and $v_{{\rm F}y}$ are rewritten as

$$\begin{cases} v_{{\rm F}x} = v_{{\rm F}X}\cos\theta\cos\varphi + v_{{\rm F}Y}\cos\theta\sin\varphi - v_{{\rm F}Z}\sin\theta \\ v_{{\rm F}y} = -v_{{\rm F}X}\sin\varphi + v_{{\rm F}Y}\cos\varphi \end{cases}, \tag{25}$$

so that

$$\begin{cases} \langle v_{{\rm F}x}^2\rangle = (\langle v_{{\rm F}X}^2\rangle\cos^2\varphi + \langle v_{{\rm F}Y}^2\rangle\sin^2\varphi)\cos^2\theta + \langle v_{{\rm F}Z}^2\rangle\sin^2\theta \\ \langle v_{{\rm F}y}^2\rangle = \langle v_{{\rm F}X}^2\rangle\sin^2\varphi + \langle v_{{\rm F}Y}^2\rangle\cos^2\varphi \\ \langle v_{{\rm F}x}v_{{\rm F}y}\rangle = (\langle v_{{\rm F}Y}^2\rangle - \langle v_{{\rm F}X}^2\rangle)\cos\theta\cos\varphi\sin\varphi \end{cases}. \tag{26}$$

The quantities $\langle\phi v_{{\rm F}x}v_{{\rm F}y}\rangle$ and $\langle\phi^2 v_{{\rm F}x}v_{{\rm F}y}\rangle$ can be expressed similarly in the crystallographic coordinates once $\phi(\mathbf{k}_{\rm F})$ is given explicitly. In particular, when $\phi(\mathbf{k}_{\rm F})$ belongs to the A_{1g} representation, the expressions for the two averages are essentially the same as Eq. (26). From Eqs. (23), (20), and (26), we realize immediately that the initial slope is isotropic when $\phi(\mathbf{k}_{\rm F})$ belongs to A_{1g} and the crystal has cubic symmetry.

The expression for B_2 is more complicated as given explicitly by Eq. (A9a). It includes Fermi-surface averages of v_{Fx}^4, $v_{Fx}^2v_{Fy}^2$, etc., and enables us to estimate the initial curvature of H_{c2} given the Fermi-surface structure.

E. H_{c2} equation

We now derive an H_{c2} equation that can be solved efficiently at all temperatures. To this end, we transform Eqs. (12a) and (12b) into algebraic equations by expanding Δ and $f^{(1)}$ in the basis functions of of Eq. (21) as[41,70]

$$\Delta(\mathbf{r}) = \sqrt{V}\sum_{N=0}^{\infty}\Delta_N\psi_{N\mathbf{q}}(\mathbf{r}), \tag{27a}$$

$$f^{(1)}(\varepsilon_n,\mathbf{k}_{\rm F},\mathbf{r}) = \sqrt{V}\sum_{N=0}^{\infty}f_N^{(1)}(\varepsilon_n,\mathbf{k}_{\rm F})\psi_{N\mathbf{q}}(\mathbf{r}). \tag{27b}$$

Let us substitute Eqs. (14) and (27) into Eqs. (12a) and (12b), multiply them by $\psi_{N\mathbf{q}}^*(\mathbf{r})$, and perform integrations over $\mathbf{r}$. Equations (12a) and (12b) are thereby transformed into

$$\sum_{N'}\mathcal{M}_{NN'}f_{N'}^{(1)} = \phi\Delta_N + \frac{\hbar}{2\tau}\langle f_N^{(1)}\rangle, \tag{28a}$$

$$\Delta_N\ln\frac{T_{c0}}{T} = -\pi T\sum_{n=-\infty}^{\infty}\left(\langle\phi f_N^{(1)}\rangle - \frac{\Delta_N}{|\varepsilon_n|}\right), \tag{28b}$$

where the matrix $\mathcal{M}$ is tridiagonal as

$$\mathcal{M}_{NN'} \equiv \tilde{\varepsilon}_n'\delta_{NN'} + \sqrt{N+1}\,\overline{\beta}^*\,\delta_{N,N'-1} - \sqrt{N}\,\overline{\beta}\,\delta_{N,N'+1}, \tag{29}$$

with

$$\overline{\beta} \equiv \frac{\hbar\overline{v}_{\rm F+}{\rm sgn}(\varepsilon_n)}{2\sqrt{2}l_{\rm c}}. \tag{30}$$

We first focus on Eq. (28a) and introduce the matrix $\mathcal{K}$ by

$$\mathcal{K}_{NN'} \equiv (\mathcal{M}^{-1})_{NN'}, \tag{31}$$

which necessarily has the same symmetry as $\mathcal{M}$,[72]

$$\begin{aligned}\mathcal{K}_{NN'}(\varepsilon_n,\overline{\beta}) &= \mathcal{K}_{N'N}(\varepsilon_n,-\overline{\beta}^*) \\ &= \mathcal{K}_{NN'}^*(-\varepsilon_n,-\overline{\beta}^*) = \mathcal{K}_{N'N}^*(-\varepsilon_n,\overline{\beta}).\end{aligned} \tag{32}$$

Using $\mathcal{K}$, Eq. (28a) is solved formally as

$$f_N^{(1)} = \sum_{N'}\mathcal{K}_{NN'}\left(\phi\Delta_{N'} + \frac{\hbar}{2\tau}\langle f_{N'}^{(1)}\rangle\right). \tag{33}$$

Taking the Fermi-surface average to obtain $\langle f_N^{(1)}\rangle$ and substituting it back into Eq. (33), we arrive at an expression for the vector $\mathbf{f}^{(1)} \equiv (f_0^{(1)}, f_1^{(1)}, f_2^{(1)}, \cdots)^{\rm T}$ as

$$\mathbf{f}^{(1)} = \left[\mathcal{K}\phi + \frac{\hbar}{2\tau}\mathcal{K}\left(\mathcal{I}-\frac{\hbar\langle\mathcal{K}\rangle}{2\tau}\right)^{-1}\langle\mathcal{K}\phi\rangle\right]\mathbf{\Delta}, \tag{34}$$

with $\mathcal{I}$ the unit matrix in the Landau-level indices and $\mathbf{\Delta} \equiv (\Delta_0,\Delta_1,\Delta_2,\cdots)^{\rm T}$.

We next substitute Eq. (34) into Eq. (28b). We thereby obtain the condition that Eq. (28b) has a nontrivial solution for $\mathbf{\Delta}$ as

$$\det\mathcal{A} = 0, \tag{35}$$

where the matrix $\mathcal{A}$ is defined by

$$\begin{aligned}\mathcal{A} = \mathcal{I}\ln\frac{T}{T_{c0}} + \pi T\sum_{n=-\infty}^{\infty}\Bigg[&\frac{\mathcal{I}}{|\varepsilon_n|} - \langle\mathcal{K}\phi^2\rangle \\ &- \frac{\hbar}{2\tau}\langle\mathcal{K}\phi\rangle\left(\mathcal{I}-\frac{\hbar\langle\mathcal{K}\rangle}{2\tau}\right)^{-1}\langle\mathcal{K}\phi\rangle\Bigg],\end{aligned} \tag{36}$$

with $\mathcal{I}$ the unit matrix in the Landau-level indices. The upper critical field B_{c2} corresponds to the highest field where Eq. (35) is satisfied, with B and H connected by Eq. (7). Put another way, B_{c2} is determined by requiring that the smallest eigenvalue of $\mathcal{A}$ be zero. Notice that $\mathcal{A}$ is Hermitian, as can

be shown by using Eq. (32), so that it can be diagonalized easily.

Equation (36) tells us that central to determining B_{c2} lies the calculation of $\mathcal{K}_{NN'}$ defined by Eqs. (29) and (31). An efficient algorithm for it was already developed in Sec. IIF of Ref. 41, which is summarized as follows. Let us define $R_N(N=0,1,2,\cdots)$ and $\overline{R}_N(N=1,2,\cdots)$ by

$$R_{N-1} = (1 + Nx^2 R_N)^{-1}, \tag{37a}$$

$$\overline{R}_{N+1} = (1 + Nx^2 \overline{R}_N)^{-1}, \quad \overline{R}_1 = 1, \tag{37b}$$

respectively, with

$$x \equiv |\overline{\beta}|/\tilde{\varepsilon}'_n. \tag{38}$$

Then $\mathcal{K}_{NN'}$ for $N \geqslant N'$ can be obtained by

$$\mathcal{K}_{NN'} = \frac{1}{\tilde{\varepsilon}'_n} \eta_N(x) \overline{\eta}_{N'}(x) \left(\frac{\overline{\beta}}{\tilde{\varepsilon}'_n} \right)^{N-N'}, \tag{39}$$

with

$$\eta_N \equiv \sqrt{N!} \prod_{k=0}^{N} R_k, \tag{40a}$$

$$\overline{\eta}_N \equiv \begin{cases} 1 & (N=0) \\ \dfrac{1}{\sqrt{N!}} \displaystyle\prod_{k=1}^{N} \dfrac{1}{\overline{R}_k} & (N \geqslant 1) \end{cases}. \tag{40b}$$

The expression of $\mathcal{K}_{NN'}$ for $N<N'$ follows immediately by Eq. (32).

As shown in Appendix II, Eqs. (40a) and (40b) can be written alternatively as

$$\begin{aligned} \eta_N(x) &\equiv \frac{2}{\sqrt{\pi N!}} \int_0^\infty \frac{s^N H_N(s)}{1+2x^2 s^2} \mathrm{e}^{-s^2} ds \\ &= \frac{1}{\sqrt{N!}} \int_0^\infty s^N \exp\left(-s - \frac{x^2}{2} s^2 \right) ds \\ &= 2^N \sqrt{\pi N!}\, z^{N+1} \mathrm{e}^{z^2} \mathrm{i}^N \operatorname{erfc}(z), \end{aligned} \tag{41a}$$

$$\begin{aligned} \overline{\eta}_N(x) &\equiv \frac{1}{\sqrt{N!}} \left(\frac{x}{\sqrt{2}i} \right)^N H_N\left(\frac{i}{\sqrt{2}x} \right) \\ &= \frac{1}{y^N \sqrt{N!}} \mathrm{e}^{-y^2/2} \left(\frac{d}{dy} \right)^N \mathrm{e}^{y^2/2} \Big|_{y=1/x}. \end{aligned} \tag{41b}$$

respectively, where $z \equiv 1/\sqrt{2}x$ and $\mathrm{i}^N \operatorname{erfc}(z)$ denotes the repeated integral of the error function.[73] The latter function $\overline{\eta}_N(x)$ is an $(N/2)$th-order [$(N-1/2)$th-order] polynomial of x^2 for $N=$even (odd).

Thus, the key quantity $\mathcal{K}_{NN'}$ is given here in a compact separable form with respect to N and N'. This is a plausible feature for performing numerical calculations, which may be considered as one of the main advantages of the present formalism over that of Langmann.[33] Our $\mathcal{K}_{00}$ in Eq. (39) is more convenient than Eq. (26) of Hohenberg and Werthamer[9] in that H_{c2} near T_c is described in terms of the lowest Landau level for arbitrary crystal structures.

Equations (35) and (36) with Eqs. (13), (15), (18)–(20), (30), and (39) are one of the main results of the paper (see also Table I). They enable us efficient calculations of H_{c2} at all temperatures based on the Fermi surfaces from *ab initio* electronic-structure calculations. They form a direct extension of the Rieck-Scharnberg equation[30] to the cases with gap anisotropy and arbitrary strength of the impurity scattering. Indeed, Eq. (41b) is written alternatively as

$$\overline{\eta}_{2N}(x) = \frac{1}{\sqrt{(2N)!}\, 2^N z^{2N}} P_N(2z^2), \tag{42}$$

with $z \equiv 1/\sqrt{2}x$, where P_N is the polynomial defined below Eq. (6) of Rieck and Scharnberg.[30] Substituting this result and the last expression of Eq. (41a) into Eq. (39), it can be checked directly that $\tilde{\varepsilon}_n \mathcal{K}_{2N'2N}$ for $N' \leqslant N$ is equal to $M_{2N'2N}$ in Eq. (6) of Rieck and Scharnberg.[30] Using this fact, one can show that the matrix $\mathcal{A}$ in Eq. (36) reduces to the corresponding matrix in Eq. (5) of Rieck and Scharnberg either (i) for the isotropic gap with arbitrary impurity scattering or (ii) in the clean limit with an arbitrary gap structure. Here we have adopted x in Eq. (38) as a variable instead of z because x remains finite at finite temperatures.

From Eq. (39) and the symmetry $\overline{\beta} \to -\overline{\beta}$ for $\mathbf{v}_\mathrm{F} \to -\mathbf{v}_\mathrm{F}$, we realize that $\langle \mathcal{K}_{2N,2N'+1} \rangle$, $\langle \mathcal{K}_{2N,2N'+1} \phi \rangle$, and $\langle \mathcal{K}_{2N,2N'+1} \phi^2 \rangle$ all vanish in the present case where the system has inversion symmetry and $\phi(\mathbf{k}_\mathrm{F})$ belongs to an even-parity representation. It, hence, follows that we only have to consider $N=$even Landau levels in the calculation of Eq. (36). To obtain a matrix element of Eq. (36), we have to perform a Fermi-surface integral for each n and perform the summation over n, which is well within the capacity of modern computers, however. Actual calculations of the smallest eigenvalue may be performed by taking only $N \leqslant N_\mathrm{cut}$ Landau levels into account, and the convergence can be checked by increasing N_cut. We can put $N_\mathrm{cut}=0$ near T_c due to Eq. (19), and must increase N_cut as the temperature is lowered. However, excellent convergence is expected at all temperatures by choosing $N_\mathrm{cut} \lesssim 20$.

III. EXTENSIONS OF THE H_{c2} EQUATION

We extend the H_{c2} equation of Sec. II in several directions.

A. *p*-wave impurity scattering

We first take p-wave impurity scattering into account. In this case, Eq. (10a) is replaced by

$$\begin{aligned} &\left(\varepsilon_n - i\mu_\mathrm{B} B + \frac{\hbar}{2\tau} \langle g \rangle + \frac{3\hbar}{2\tau_1} \hat{\mathbf{k}}'_\mathrm{F} \cdot \langle \hat{\mathbf{k}}'_\mathrm{F} g \rangle' + \frac{1}{2} \hbar \mathbf{v}_\mathrm{F} \cdot \boldsymbol{\partial} \right) f \\ &= \left(\phi \Delta + \frac{\hbar}{2\tau} \langle f \rangle + \frac{3\hbar}{2\tau_1} \hat{\mathbf{k}}_\mathrm{F} \cdot \langle \hat{\mathbf{k}}'_\mathrm{F} f \rangle' \right) g, \end{aligned} \tag{43}$$

where $\langle \hat{\mathbf{k}}'_\mathrm{F} g \rangle' \equiv \langle \hat{\mathbf{k}}'_\mathrm{F} g(\varepsilon_n, \mathbf{k}'_\mathrm{F}, \mathbf{r}) \rangle'$, for example, and $\hat{\mathbf{k}}_\mathrm{F} \equiv \mathbf{k}_\mathrm{F} / \langle k_\mathrm{F}^2 \rangle^{1/2}$. Notice that $\hat{\mathbf{k}}_\mathrm{F}$ is not a unit vector in general.

Linearizing Eq. (43) with respect to Δ, we obtain

$$\left(\tilde{\varepsilon}_n' + \frac{\mathrm{sgn}(\varepsilon_n)}{2}\hbar\mathbf{v}_\mathrm{F}\cdot\boldsymbol{\partial}\right)f^{(1)} = \phi\Delta + \frac{\hbar}{2\tau}\langle f^{(1)}\rangle + \frac{3\hbar}{2\tau_1}\hat{\mathbf{k}}_\mathrm{F}\cdot\langle\hat{\mathbf{k}}_\mathrm{F}' f^{(1)}\rangle', \tag{44}$$

with $\tilde{\varepsilon}_n'$ defined by Eq. (13).

First of all, we derive expressions for T_c at $H=0$, the coefficients (c_1,c_2) in Eq. (16), and B_{c2} near T_c up to the first order in $1-t$, based on Eq. (44) and following the procedure in Sec. A. It turns out that we only need a change of the definition of χ_{ij} from Eq. (20) into

$$\chi_{ij} \equiv \frac{24(\pi T_c)^3}{7\zeta(3)\langle v_\mathrm{F}^2\rangle}\sum_{n=0}^{\infty}\frac{1}{\tilde{\varepsilon}_n^3}\left[\left\langle v_{\mathrm{F}i}v_{\mathrm{F}j}\left|\phi + \frac{\langle\phi\rangle}{2\tau\varepsilon_n/\hbar}\right|^2\right\rangle + \frac{3}{2\tau_1\tilde{\varepsilon}_n/\hbar}(\mathcal{P}^\dagger\mathcal{Q}^{-1}\mathcal{P})_{ij}\right], \tag{45}$$

where the matrices $\mathcal{P}$ and $\mathcal{Q}$ are defined by

$$\mathcal{P}_{ij} \equiv \left\langle\left(\phi + \frac{\langle\phi\rangle}{2\tau|\varepsilon_n|/\hbar}\right)\hat{k}_{\mathrm{F}i}v_{\mathrm{F}j}\right\rangle, \tag{46a}$$

$$\mathcal{Q}_{ij} \equiv \delta_{ij} - \frac{3\hbar}{2\tau_1\tilde{\varepsilon}_n}\langle\hat{k}_{\mathrm{F}i}\hat{k}_{\mathrm{F}j}\rangle. \tag{46b}$$

Then T_c, (c_1,c_2), and B_1 in Eq. (22) are given by the same equations, i.e., Eqs. (A5), (19), and (23), respectively.

Using Eqs. (14) and (27), we next transform Eq. (44) into an algebraic equation. The resulting equation can solved in the same way as Eq. (33) to yield

$$\mathbf{f}^{(1)} = \mathcal{K}\left(\phi\boldsymbol{\Delta} + \frac{\hbar}{2\tau}\langle\mathbf{f}^{(1)}\rangle + \frac{3\hbar}{2\tau_1}\hat{\mathbf{k}}_\mathrm{F}\cdot\langle\hat{\mathbf{k}}_\mathrm{F}'\mathbf{f}^{(1)}\rangle'\right), \tag{47}$$

where $\mathcal{K}$ is given by Eq. (39). It is convenient to introduce the quantities

$$p_0 \equiv \sqrt{\frac{\hbar}{2\tau}}, \quad p_j \equiv \sqrt{\frac{3\hbar}{2\tau_1}}\hat{k}_{\mathrm{F}j}\ (j=x,y,z). \tag{48}$$

Then from Eq. (47), we obtain self-consistent equations for $\langle p_0^*\mathbf{f}^{(1)}\rangle$ and $\langle p_j^*\mathbf{f}^{(1)}\rangle$ as

$$\begin{bmatrix}\langle p_0^*\mathbf{f}^{(1)}\rangle\\ \langle p_x^*\mathbf{f}^{(1)}\rangle\\ \langle p_y^*\mathbf{f}^{(1)}\rangle\\ \langle p_z^*\mathbf{f}^{(1)}\rangle\end{bmatrix} = \mathcal{W}\begin{bmatrix}\langle p_0^*\mathcal{K}\phi\rangle\boldsymbol{\Delta}\\ \langle p_x^*\mathcal{K}\phi\rangle\boldsymbol{\Delta}\\ \langle p_y^*\mathcal{K}\phi\rangle\boldsymbol{\Delta}\\ \langle p_z^*\mathcal{K}\phi\rangle\boldsymbol{\Delta}\end{bmatrix}, \tag{49}$$

where the matrix $\mathcal{W}$ is defined by

$$\mathcal{W} \equiv \begin{bmatrix}\mathcal{I}-\langle|p_0|^2\mathcal{K}\rangle & -\langle p_0^*p_x\mathcal{K}\rangle & -\langle p_0^*p_y\mathcal{K}\rangle & -\langle p_0^*p_z\mathcal{K}\rangle\\ -\langle p_x^*p_0\mathcal{K}\rangle & \mathcal{I}-\langle|p_x|^2\mathcal{K}\rangle & -\langle p_x^*p_y\mathcal{K}\rangle & -\langle p_x^*p_z\mathcal{K}\rangle\\ -\langle p_y^*p_0\mathcal{K}\rangle & -\langle p_y^*p_x\mathcal{K}\rangle & \mathcal{I}-\langle|p_y|^2\mathcal{K}\rangle & -\langle p_y^*p_z\mathcal{K}\rangle\\ -\langle p_z^*p_0\mathcal{K}\rangle & -\langle p_z^*p_x\mathcal{K}\rangle & -\langle p_z^*p_y\mathcal{K}\rangle & \mathcal{I}-\langle|p_z|^2\mathcal{K}\rangle\end{bmatrix}^{-1}. \tag{50}$$

The complex conjugations * in Eqs. (49) and (50) are not necessary here but for a later convenience. Not the symmetry $\mathcal{W}_{lm}^*(\varepsilon_n,\overline{\beta}) = \mathcal{W}_{ml}(-\varepsilon_n,\overline{\beta})$ in the matrix elements of $\mathcal{W}$, as seen from Eq. (32). Using Eq. (49) in Eq. (47), we obtain an explicit expression for $\mathbf{f}^{(1)}$ as

$$\mathbf{f}^{(1)} = \mathcal{K}\phi\boldsymbol{\Delta} + [p_0\mathcal{K}p_x\mathcal{K}p_y\mathcal{K}p_z\mathcal{K}]\mathcal{W}\begin{bmatrix}\langle p_0^*\mathcal{K}\phi\rangle\\ \langle p_x^*\mathcal{K}\phi\rangle\\ \langle p_y^*\mathcal{K}\phi\rangle\\ \langle p_z^*\mathcal{K}\phi\rangle\end{bmatrix}\boldsymbol{\Delta}. \tag{51}$$

Finally, let us substitute Eq. (51) into Eq. (28b). We thereby find that Eq. (36) is replaced by

$$\mathcal{A} = \mathcal{I}\ln\frac{T}{T_{c0}} + \pi T\sum_{n=-\infty}^{\infty}\left\{\frac{\mathcal{I}}{|\varepsilon_n|} - \langle\mathcal{K}\phi^2\rangle - [\langle p_0\mathcal{K}\phi\rangle\langle p_x\mathcal{K}\phi\rangle \times\langle p_y\mathcal{K}\phi\rangle\langle p_z\mathcal{K}\phi\rangle]\mathcal{W}\begin{bmatrix}\langle p_0^*\mathcal{K}\phi\rangle\\ \langle p_x^*\mathcal{K}\phi\rangle\\ \langle p_y^*\mathcal{K}\phi\rangle\\ \langle p_z^*\mathcal{K}\phi\rangle\end{bmatrix}\right\}. \tag{52}$$

As before, H_{c2} is determined by requiring that the smallest eigenvalue of Eq. (52) be zero. This $\mathcal{A}$ is Hermitian, as can be shown by using Eq. (32) and $\mathcal{W}_{lm}^*(\varepsilon_n,\overline{\beta}) \equiv \mathcal{W}_{ml}(-\varepsilon_n,\overline{\beta})$. Thus, Eq. (52) can be diagonalized easily.

It is straightforward to extend Eq. (52) to a more general impurity scattering with the $\mathbf{k}_F$-dependent relaxation time $\tau(\mathbf{k}_F,\mathbf{k}_F')$. To this end, we apply the procedure of Eqs. (2)–(5) to $1/\tau(\mathbf{k}_F,\mathbf{k}_F')$ to expand it as

$$\frac{1}{\tau(\mathbf{k}_F,\mathbf{k}_F')}=\sum_{\Gamma j\gamma}\frac{\eta_\gamma^{(\Gamma j)}(\mathbf{k}_F)\eta_\gamma^{(\Gamma j)*}(\mathbf{k}_F)}{\tau^{(\Gamma j)}}, \tag{53}$$

where $1/\tau^{(\Gamma j)}$ and $\eta_\gamma^{(\Gamma j)}(\mathbf{k}_F)$ denote an eigenvalue and its eigenfunction, respectively. We then realize that

$$p_\gamma^{(\Gamma j)}\equiv\sqrt{\frac{\hbar}{2\tau^{(\Gamma j)}}}\eta_\gamma^{(\Gamma j)}(\mathbf{k}_F) \tag{54}$$

substitutes for p_0 and p_j in Eq. (52).

B. Spin-orbit impurity scattering

It was noticed by Werthamer *et al.*[7] and Maki[8] that, for high-field superconducting alloys with short mean-free paths, Pauli paramagnetism has to be incorporated simultaneously with spin-orbit impurity scattering. They presented a theory valid for $\tau\ll\tau_{so}$, where τ_{so} is spin-orbit scattering time. It was later generalized by Rieck *et al.*[31] for an arbitrary value of τ_{so}. This effect can also be taken into account easily in the formulation.

In the presence of spin-orbit impurity scattering, Eq. (10a) is replaced by

$$\left(\varepsilon_n-i\mu_B B+\frac{\hbar}{2\tau}\langle g\rangle+\frac{\hbar c_{so}}{2\tau_{so}}\langle|\hat{\mathbf{k}}_F\times\hat{\mathbf{k}}_F'|^2 g\rangle'+\frac{1}{2}\hbar\mathbf{v}_F\cdot\boldsymbol{\partial}\right)f$$
$$=\left(\phi\Delta+\frac{\hbar}{2\tau}\langle f\rangle+\frac{\hbar c_{so}}{2\tau_{so}}\langle|\hat{\mathbf{k}}_F\times\hat{\mathbf{k}}_F'|^2 f\rangle'\right)g, \tag{55}$$

with $c_{so}\equiv 1/\langle\langle|\hat{\mathbf{k}}_F\times\hat{\mathbf{k}}_F'|^2\rangle'\rangle$. To simplify the notations and make the argument transparent, it is useful to introduce the quantities

$$p_0\equiv\sqrt{\frac{\hbar}{2\tau}},\quad p_{ij}\equiv\sqrt{\frac{\hbar c_{so}}{2\tau_{so}}}(\hat{k}_F^2\delta_{ij}-\hat{k}_{Fi}\hat{k}_{Fj}), \tag{56a}$$

$$q_0\equiv\sqrt{\frac{\hbar}{2\tau}},\quad q_{ij}\equiv\sqrt{\frac{\hbar c_{so}}{2\tau_{so}}}\hat{k}_{Fi}\hat{k}_{Fj}(2-\delta_{ij}), \tag{56b}$$

and the vectors

$$\mathbf{p}\equiv(p_0,p_{xx},p_{yy},p_{zz},p_{xy},p_{yz},p_{zx})^T, \tag{57a}$$

$$\mathbf{q}\equiv(q_0,q_{xx},q_{yy},q_{zz},q_{xy},q_{yz},q_{zx})^T. \tag{57b}$$

Then Eq. (55) linearized with respect to Δ is written in terms of Eq. (57) as

$$\left(\tilde{\varepsilon}_n'+\frac{\mathrm{sgn}(\varepsilon_n)}{2}\hbar\mathbf{v}_F\cdot\boldsymbol{\partial}\right)f^{(1)}=\phi\Delta+\mathbf{p}\cdot\langle\mathbf{q}f^{(1)}\rangle, \tag{58}$$

where $\tilde{\varepsilon}_n'$ is defined by

$$\tilde{\varepsilon}_n'\equiv\tilde{\varepsilon}_n-i\mu_B B\,\mathrm{sgn}(\varepsilon_n),\quad \tilde{\varepsilon}_n\equiv|\varepsilon_n|+\mathbf{p}\cdot\langle\mathbf{q}\rangle. \tag{59}$$

Note $\mathbf{p}\cdot\langle\mathbf{q}\rangle=\langle\mathbf{p}\rangle\cdot\mathbf{q}$.

It follows from the procedure in Sec. III A that T_c at $H=0$ satisfies

$$\ln\frac{T_{c0}}{T_c}=2\pi T_c\sum_{n=0}^{\infty}\left[\frac{1}{\varepsilon_n}-\left\langle\frac{\phi^2}{\tilde{\varepsilon}_n}\right\rangle-\left\langle\frac{\mathbf{p}^T\phi}{\tilde{\varepsilon}_n}\right\rangle\mathcal{Q}^{-1}\left\langle\frac{\mathbf{q}\phi}{\tilde{\varepsilon}_n}\right\rangle\right], \tag{60}$$

where the matrix $\mathcal{Q}$ is defined by $(r,s=0,xx,\cdots,zx)$

$$\mathcal{Q}_{rs}=\delta_{rs}-\left\langle\frac{q_r p_s}{\tilde{\varepsilon}_n}\right\rangle. \tag{61}$$

Also, χ_{ij} in Eq. (20) should be modified into

$$\chi_{ij}\equiv\frac{24(\pi T_c)^3}{7\zeta(3)\langle v_F^2\rangle}\sum_{n=0}^{\infty}\left\langle v_{Fi}v_{Fj}\left[\phi+\left\langle\frac{\mathbf{p}^T\phi}{\tilde{\varepsilon}_n}\right\rangle\mathcal{Q}^{-1}\mathbf{q}\right]\right.$$
$$\left.\times\left[\phi+\mathbf{p}^T\mathcal{Q}^{-1}\left\langle\frac{\mathbf{q}\phi}{\tilde{\varepsilon}_n}\right\rangle\right]\right\rangle. \tag{62}$$

Finally, R in Eq. (24) is replaced by

$$R=1-2\pi T_c\sum_{n=0}^{\infty}\left[\left\langle\frac{\phi^2\mathbf{p}\cdot\langle\mathbf{q}\rangle}{\tilde{\varepsilon}_n^2}\right\rangle+\left\langle\frac{\mathbf{p}\cdot\langle\mathbf{q}\rangle\mathbf{p}^T\phi}{\tilde{\varepsilon}_n^2}\right\rangle\mathcal{Q}^{-1}\left\langle\frac{\mathbf{q}\phi}{\tilde{\varepsilon}_n}\right\rangle\right.$$
$$-\varepsilon_n\left\langle\frac{\mathbf{p}^T\phi}{\tilde{\varepsilon}_n}\right\rangle\mathcal{Q}^{-1}\left\langle\frac{\mathbf{q}\phi}{\tilde{\varepsilon}_n^2}\right\rangle$$
$$\left.-\varepsilon_n\left\langle\frac{\mathbf{p}^T\phi}{\tilde{\varepsilon}_n}\right\rangle\mathcal{Q}^{-1}\left\langle\frac{\mathbf{q}^T\mathbf{p}}{\tilde{\varepsilon}_n^2}\right\rangle\mathcal{Q}^{-1}\left\langle\frac{\mathbf{q}\phi}{\tilde{\varepsilon}_n}\right\rangle\right]. \tag{63}$$

With the above modifications, T_c, (c_1,c_2), and B_1 in Eq. (22) are given by Eqs. (A5), (19), and (23), respectively.

We now transform Eq. (58) into an algebraic equation by using Eqs. (14) and (27). The resulting equation can be solved in the same way as Eq. (33). We thereby obtain

$$\mathbf{f}^{(1)}=\mathcal{K}\phi\boldsymbol{\Delta}+\sum_r p_r\mathcal{K}\langle q_r\mathbf{f}^{(1)}\rangle, \tag{64}$$

where $\mathcal{K}$ is given by Eq. (39) with $\overline{\varepsilon_n^{\gamma}}$ replaced by Eq. (59). From Eq. (64), we obtain self-consistent equations for $\langle q_0\mathbf{f}^{(1)}\rangle$ and $\langle q_{ij}\mathbf{f}^{(1)}\rangle$ as

$$\begin{bmatrix}\langle q_0\mathbf{f}^{(1)}\rangle\\ \langle q_{xx}\mathbf{f}^{(1)}\rangle\\ \langle q_{yy}\mathbf{f}^{(1)}\rangle\\ \langle q_{zz}\mathbf{f}^{(1)}\rangle\\ \langle q_{xy}\mathbf{f}^{(1)}\rangle\\ \langle q_{yz}\mathbf{f}^{(1)}\rangle\\ \langle q_{zx}\mathbf{f}^{(1)}\rangle\end{bmatrix}=\mathcal{W}\begin{bmatrix}\langle q_0\mathcal{K}\phi\rangle\boldsymbol{\Delta}\\ \langle q_{xx}\mathcal{K}\phi\rangle\boldsymbol{\Delta}\\ \langle q_{yy}\mathcal{K}\phi\rangle\boldsymbol{\Delta}\\ \langle q_{zz}\mathcal{K}\phi\rangle\boldsymbol{\Delta}\\ \langle q_{xy}\mathcal{K}\phi\rangle\boldsymbol{\Delta}\\ \langle q_{yz}\mathcal{K}\phi\rangle\boldsymbol{\Delta}\\ \langle q_{zx}\mathcal{K}\phi\rangle\boldsymbol{\Delta}\end{bmatrix}, \tag{65}$$

where the matrix $\mathcal{W}$ is defined by

$$\mathcal{W} \equiv \begin{bmatrix} \mathcal{I} - \langle q_0 p_0 \mathcal{K} \rangle & -\langle q_0 p_{xx} \mathcal{K} \rangle & -\langle q_0 p_{yy} \mathcal{K} \rangle & \cdots \\ -\langle q_{xx} p_0 \mathcal{K} \rangle & \mathcal{I} - \langle q_{xx} p_{xx} \mathcal{K} \rangle & -\langle q_{xx} p_{yy} \mathcal{K} \rangle & \cdots \\ -\langle q_{yy} p_0 \mathcal{K} \rangle & -\langle q_{yy} p_{xx} \mathcal{K} \rangle & \mathcal{I} - \langle q_{yy} p_{yy} \mathcal{K} \rangle & \cdots \\ -\langle q_{zz} p_0 \mathcal{K} \rangle & -\langle q_{zz} p_{xx} \mathcal{K} \rangle & -\langle q_{zz} p_{yy} \mathcal{K} \rangle & \cdots \\ -\langle q_{xy} p_0 \mathcal{K} \rangle & -\langle q_{xy} p_{xx} \mathcal{K} \rangle & -\langle q_{xy} p_{yy} \mathcal{K} \rangle & \cdots \\ -\langle q_{yz} p_0 \mathcal{K} \rangle & -\langle q_{yz} p_{xx} \mathcal{K} \rangle & -\langle q_{yz} p_{yy} \mathcal{K} \rangle & \cdots \\ -\langle q_{zx} p_0 \mathcal{K} \rangle & -\langle q_{zx} p_{xx} \mathcal{K} \rangle & -\langle q_{zx} p_{yy} \mathcal{K} \rangle & \cdots \end{bmatrix}^{-1}. \tag{66}$$

Using Eq. (65) in Eq. (64), we obtain an explicit expression for $\mathbf{f}^{(1)}$ as

$$\begin{aligned} \mathbf{f}^{(1)} &= \mathcal{K}\phi\boldsymbol{\Delta} + [p_0 \mathcal{K} p_{xx} \mathcal{K} p_{yy} \mathcal{K} \cdots] \mathcal{W} \begin{bmatrix} \langle q_0 \mathcal{K} \phi \rangle \\ \langle q_{xx} \mathcal{K} \phi \rangle \\ \langle q_{yy} \mathcal{K} \phi \rangle \\ \vdots \end{bmatrix} \boldsymbol{\Delta} \\ &= \mathcal{K}\phi\boldsymbol{\Delta} + [q_0 \mathcal{K} q_{xx} \mathcal{K} q_{yy} \mathcal{K} \cdots] \mathcal{W}^\dagger \begin{bmatrix} \langle p_0 \mathcal{K} \phi \rangle \\ \langle p_{xx} \mathcal{K} \phi \rangle \\ \langle p_{yy} \mathcal{K} \phi \rangle \\ \vdots \end{bmatrix} \boldsymbol{\Delta}, \end{aligned} \tag{67}$$

with $\mathcal{W}^\dagger$ defined by $[\mathcal{W}^\dagger(\varepsilon_n, \overline{\beta})]_{lm} \equiv \mathcal{W}^*_{ml}(-\varepsilon_n, \overline{\beta})$. The latter expression originates from the self-consistency equations for $\langle p_0 \mathbf{f}^{(1)} \rangle$ and $\langle p_{ij} \mathbf{f}^{(1)} \rangle$ similar to Eq. (65). Finally, let us substitute Eq. (67) into Eq. (28b). We thereby find that Eq. (36) is replaced by

$$\begin{aligned} \mathcal{A} &= \mathcal{I} \ln \frac{T}{T_{c0}} + \pi T \sum_{n=-\infty}^{\infty} \left\{ \frac{\mathcal{I}}{|\varepsilon_n|} - \langle \mathcal{K} \phi^2 \rangle \right. \\ &\quad \left. - [\langle p_0 \mathcal{K} \phi \rangle \langle p_{xx} \mathcal{K} \phi \rangle \langle p_{yy} \mathcal{K} \phi \rangle \cdots] \mathcal{W} \begin{bmatrix} \langle q_0 \mathcal{K} \phi \rangle \\ \langle q_{xx} \mathcal{K} \phi \rangle \\ \langle q_{yy} \mathcal{K} \phi \rangle \\ \cdots \end{bmatrix} \right\} \\ &= \mathcal{I} \ln \frac{T}{T_{c0}} + \pi T \sum_{n=-\infty}^{\infty} \left\{ \frac{\mathcal{I}}{|\varepsilon_n|} - \langle \mathcal{K} \phi^2 \rangle \right. \\ &\quad \left. - [\langle q_0 \mathcal{K} \phi \rangle \langle q_{xx} \mathcal{K} \phi \rangle \langle q_{yy} \mathcal{K} \phi \rangle \cdots] \mathcal{W}^\dagger \begin{bmatrix} \langle p_0 \mathcal{K} \phi \rangle \\ \langle p_{xx} \mathcal{K} \phi \rangle \\ \langle p_{yy} \mathcal{K} \phi \rangle \\ \cdots \end{bmatrix} \right\}. \end{aligned} \tag{68}$$

As before, H_{c2} is determined by requiring that the smallest eigenvalue of Eq. (68) be zero. This $\mathcal{A}$ is Hermitian, as can be shown by using Eq. (32) and $[\mathcal{W}^\dagger(\varepsilon_n, \overline{\beta})]_{lm} \equiv \mathcal{W}^*_{ml}(-\varepsilon_n, \overline{\beta})$, which can be diagonalized easily.

C. Strong electron-phonon interactions

We finally consider the effects of strong electron-phonon interactions within the framework of the Eliashberg theory.[61,62] We adopt the notations used by Allen and. Mitrović[62] except the replacement $Z\Delta \to \Delta$.

The Eilenberger equations were extended by Teichler[74] to include the strong-coupling effects. They can also be derived directly from the equations given by Allen and B. Mitrović[62] by carrying out the "ξ integration"[66] as

$$\left(Z\varepsilon_n - i\mu_B B + \frac{\hbar}{2\tau}\langle g \rangle + \frac{1}{2}\hbar \mathbf{v}_F \cdot \boldsymbol{\partial} \right) f = \left(\Delta\phi + \frac{\hbar}{2\tau}\langle f \rangle \right) g, \tag{69a}$$

$$\Delta(\varepsilon_n, \mathbf{r}) = \pi T \sum_{n'=-n_{c0}}^{n_{c0}} [\lambda(\varepsilon_n - \varepsilon_{n'}) - \mu^*] \langle \phi(\mathbf{k}_F) f(\varepsilon_{n'}, \mathbf{k}_F, \mathbf{r}) \rangle, \tag{69b}$$

$$Z(\varepsilon_n, \mathbf{k}_F) = 1 + \frac{\pi T}{\varepsilon_n} \sum_{n'=-n_{c0}}^{n_{c0}} \langle \lambda(\mathbf{k}_F, \mathbf{k}'_F, \varepsilon_n - \varepsilon_{n'}) g(\varepsilon_{n'}, \mathbf{k}'_F, \mathbf{r}) \rangle', \tag{69c}$$

where n_{c0} corresponds to the Matsubara frequency about five times as large as the Debye frequency.[62] We have retained full $\mathbf{k}_F$ dependence of λ in Eq. (69c) because the contribution from other pairing channels, which may be negligible for the pair potential, can be substantial for the renormalization factor Z.

We linearize Eqs. (69) with respect to Δ and repeat the procedure in Sec. A up to the zeroth order in $1-t$. It then follows that T_c at $H=0$ is determined by the condition that the smallest eigenvalue of the following matrix be zero:

$$\begin{aligned} \mathcal{A}^{(0)}_{nn'} \equiv \delta_{nn'} - \pi T [\lambda(\varepsilon_n - \varepsilon_{n'}) - \mu^*] \left[\left\langle \frac{\phi^2}{\tilde{\varepsilon}_{n'}} \right\rangle \right. \\ \left. + \frac{\hbar}{2\tau} \left\langle \frac{\phi}{\tilde{\varepsilon}_{n'}} \right\rangle^2 \left\langle \frac{\tilde{\varepsilon}_{n'}}{Z^{(0)}_{n'} |\varepsilon_{n'}|} \right\rangle \right], \end{aligned} \tag{70}$$

where $Z^{(0)}$ is given by

$$Z^{(0)}(\varepsilon_n, \mathbf{k}_F) = 1 + \frac{\pi T}{\varepsilon_n} \sum_{n'=-n_{c0}}^{n_{c0}} \langle \lambda(\mathbf{k}_F, \mathbf{k}'_F, \varepsilon_n - \varepsilon_{n'}) \rangle' \, \mathrm{sgn}(\varepsilon_{n'}), \tag{71}$$

and $\tilde{\varepsilon}_n$ is defined together with $\tilde{\varepsilon}'_n$ by

$$\tilde{\varepsilon}_n \equiv Z^{(0)} |\varepsilon_n| + \frac{\hbar}{2\tau}, \quad \tilde{\varepsilon}'_n \equiv \tilde{\varepsilon}_n - i\mu_B B \, \mathrm{sgn}(\varepsilon_n). \tag{72}$$

We next fix (c_1, c_2) in Eq. (16) conveniently. For the weak-coupling model, we have fixed it by using Eq. (A6) near T_c

so that the coefficient of aa vanishes, i.e., there is no mixing of higher Landau levels in the H_{c2} equation near T_c. However, the coefficient of aa in the corresponding strong-coupling equation becomes frequency dependent. It, hence, follows that even near T_c there is no choice for (c_1, c_2), which prevents mixing of higher Landau levels from the H_{c2} equation. We here adopt the weak-coupling expression in Eq. (19).

We now consider the H_{c2} equation and repeat the same calculations as those in Sec. II B. We thereby find that Eq. (36) is replaced by

$$\mathcal{A}_{nN,n'N'} = \delta_{nn'}\delta_{NN'} - \pi T[\lambda(\varepsilon_n - \varepsilon_{n'}) - \mu^*]\Bigg[\langle \mathcal{K}'\phi^2\rangle + \frac{\hbar}{2\tau}\langle \mathcal{K}'\phi\rangle\left(\mathcal{I} - \frac{\hbar\langle \mathcal{K}'\rangle}{2\tau}\right)^{-1}\langle \mathcal{K}'\phi\rangle\Bigg]_{NN'}, \quad (73)$$

where $\mathcal{K}' \equiv \mathcal{K}(\varepsilon_{n'}, \overline{\beta})$ which also has $\mathbf{k}_F$ dependence through $Z^{(0)\prime} = Z^{(0)}(\varepsilon_{n'}, \mathbf{k}_F)$. As before, H_{c2} is determined by requiring that the smallest eigenvalue of Eq. (73) be zero.

We may alternatively use, instead of Eq. (73), the matrix

$$\mathcal{A}'_{nN,n'N'} = (\lambda - \mu^*)^{-1}_{nn'}\delta_{NN'} - \delta_{nn'}\pi T\Bigg[\langle \mathcal{K}\phi^2\rangle + \frac{\hbar}{2\tau}\langle \mathcal{K}\phi\rangle\left(\mathcal{I} - \frac{\hbar\langle \mathcal{K}\rangle}{2\tau}\right)^{-1}\langle \mathcal{K}\phi\rangle\Bigg]_{NN'}, \quad (74)$$

where $(\lambda - \mu^*)^{-1}$ denotes inverse matrix of $\lambda - \mu^*$. It is Hermitian for $\mu_B B \to 0$, and also acquire the property by combining $n > 0$ and $n < 0$ elements.

IV. MODEL CALCULATIONS

We now present results of a model calculation based on the formalism developed above. We restrict ourselves to the weak-coupling model of Sec. II with an isotropic gap, no impurities, and no Pauli paramagnetism. As for the energy-band structure, we adopt a tight-binding model in the simple cubic lattice whose dispersion is given by

$$\varepsilon_{\mathbf{k}} = -2t\{\cos(k_x a) + \cos(k_y a) + \cos(k_z a)\}. \quad (75)$$

Here a denotes lattice spacing of the cubic unit cell and t is the nearest-neighbor transfer integral. We set $t = a = 1$ in the following. The corresponding Fermi surfaces are plotted in Fig. 1 for various values of the Fermi energy ε_F. For $\varepsilon_F \approx -6$, i.e., near the bottom of the band, the Fermi surface is almost spherical with slight distortion due to the cubic symmetry. As ε_F increases, the cubic distortion is gradually enhanced. Then at $\varepsilon_F = -2$, the Fermi surface touches the Brillouin-zone boundary at $\mathbf{k}_X \equiv (0, 0, \pm\pi), (0, \pm, \pi, 0), (\pm\pi, 0, 0)$. Above this critical Fermi energy, the topology of the Fermi surface changes, as shown in Fig. 1(c). It is interesting to see how such a topological change of the Fermi surface affects H_{c2}.

We computed H_{c2} based on Eq. (35) in the clean limit without Pauli paramagnetism. The Fermi-surface average in Eq. (36) was performed by two different methods. For general values of ε_F, we used the linear tetrahedron method, which is applicable to any structure of the Fermi surface. In this method, the irreducible Brillouin zone is divided into a collection of small tetrahedra. From each tetrahedron that intersects the Fermi surface, a segment of the Fermi surface is obtained as a polygon by a linear interpolation of the energy band. Numerical integrations over the Fermi surface were then performed as a sum over those polygons. Another description of the Fermi surface is possible for $\varepsilon_F < -2$, where we can adopt the polar coordinate $\mathbf{k} = (k\sin\theta\cos\phi, k\sin\theta\sin\phi, k\cos\theta)$, and the Fermi surface $k_F = k_F(\theta, \phi)$ is obtained by solving the equation $\varepsilon_{\mathbf{k}} = \varepsilon_F$ numerically for each (θ, ϕ). An integration over the Fermi surface is then performed by using the variables (θ, ϕ). We performed both types of calculations to check the numerical convergence of the tetrahedron method. Excellent agreements were achieved generally by using 3375 tetrahedrons. An exception is the region $\varepsilon_F \approx -2$, where a larger number of tetrahedrons was necessary due to the singularity around $\mathbf{k}_X$.

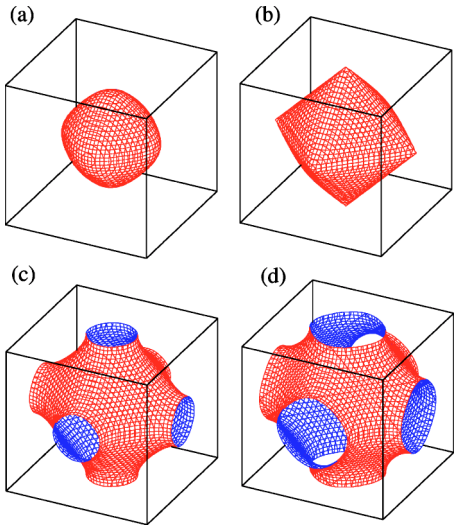

FIG. 1. Fermi surfaces of the tight-binding model in the simple cubic lattice. The Fermi energies are (a) $\varepsilon_F = -3$, (b) -2, (c) -1, and (d) 0.

The infinite matrix $\mathcal{A}_{NN'}$ in Eq. (36) was approximated by a finite matrix of $N, N' \leqslant N_{cut}$, and the convergence was checked by increasing N_{cut}. The choice $N_{cut} = 0$ is sufficient for $T \lesssim T_c$, and it was found numerically that $N_{cut} = 8$ yields enough convergence for all field directions at the lowest temperatures. It was also found that higher Landau levels of $N \geqslant 1$ contribute to H_{c2} by only 4% even at $T/T_c = 0.05$. Thus, the lowest-Landau-level approximation to the pair potential is excellent for this cubic lattice. This is not generally the case, however, and the contribution of higher Landau levels can be considerable for low-symmetry crystals, as will be reported elsewhere.[75]

Before presenting any detailed results, it is worth noting that the GL equations,[1,2] where the anisotropy enters only through the effective-mass tensor, cannot explain possible anisotropy of H_{c2} in cubic symmetry, as already pointed out by Hohenberg and Werthamer.[9] This GL theory is valid near T_c so that the upper critical field for $T \lesssim T_c$ should be isotro-

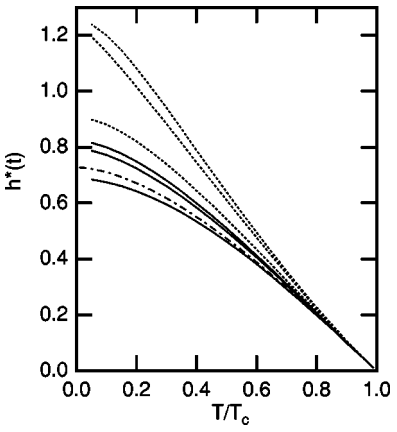

FIG. 2. Curves of the reduced critical field $h_d^*(t)$ for the cubic tight-binding model with $\varepsilon_F=-2.02$ (dotted lines), $\varepsilon_F=-3$ (solid lines), and $\varepsilon_F\to-6$ (i.e., the spherical Fermi surface; dash-dotted line). The field directions are $d=[111]$, [110], and [100] from top to bottom in each case.

pic in the present model. The anisotropy of H_{c2} in cubic symmetry emerges gradually at lower temperatures, as seen below.

We calculated the reduced critical field $h*(t)$ defined by Eq. (1) for the magnetic field directions $d=[100]$, [110], and [111]; we denote them as $h_d^*(t)$. Figure 2 presents $h_d^*(t)$ for $\varepsilon_F=-3$ and -2.02 as a function of $t=T/T_c$. For $\varepsilon_F=-3$, $h*(t)$ is almost isotropic for $t\gtrsim 0.8$ and cannot be distinguished from the curve for the spherical Fermi surface. At lower temperatures, the anisotropy appears gradually. Whereas $h_{[100]}^*(t)$ is reduced from the value for the spherical Fermi surface, $h_{[111]}^*(t)$ and $h_{[110]}^*(t)$ are enhanced due to the cubic distortion of the Fermi surface. At $t=0.05$, $h_{[111]}^*(t)$ and $h_{[110]}^*(t)$ are larger than $h_{[100]}^*(t)$ by 19% and 15%, respectively. In another case $\varepsilon_F=-2.02$ where the Fermi surface nearly touches the Brillouin zone boundary, $h_d^*(t)$ are remarkably enhanced for all field directions. Especially, $h_{[111]}^*(t)$ and $h_{[110]}^*(t)$ at low temperatures exhibit values about 60–70% larger than those for the spherical Fermi surface.

At $\varepsilon_F=-3$, $h_{[111]}^*(t)$ and $h_{[110]}^*(t)$ near T_c show small upward curvature, whereas $h_{[100]}^*(t)$ remains almost identical with the curve for the spherical Fermi surface. This difference may be quantified by the ratio B_2/B_1 defined in Eq. (22). It was numerically evaluated by using the Fermi velocity on the Fermi surface and shown in Table II. The values for the directions [110] and [111] are larger than 0.13 for the spherical Fermi surface. Thus, calculated B_2/B_1 values well

TABLE II. The ratio B_2/B_1 for the field directions [100], [110], and [111] in the cases $\varepsilon_\mathbf{F}=-3$ and -2.02. The quantities B_1 and B_2 are defined in Eq. (22). The values should be compared with 0.13 for the spherical Fermi surface.

ε_F	[100]	[110]	[111]
−3	0.08	0.27	0.33
−2.02	0.44	0.78	0.90

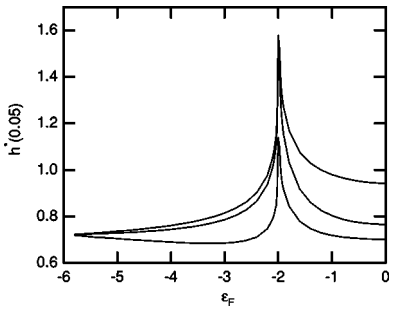

FIG. 3. The reduced upper critical field $h_d^*(t)$ at $t=0.05$ as a function of the Fermi energy ε_F. The field directions are $d=[111]$, [110], and [100] from top to bottom, respectively.

describe the difference in $h*(t)$ for $t\lesssim 1$ among field directions. The upward curvature is more and more pronounced as the Fermi surface approaches the Brillouin zone boundary, as can be seen clearly in Fig. 2 for $\varepsilon_F=-2.02$. The corresponding ratio B_2/B_1 for the [110] and [111] directions are about three times larger than those for $\varepsilon_F=-3$. Thus, the present calculation clearly indicates that the Fermi surface anisotropy can be a main source of the upward curvature in H_{c2} near T_c.

In Fig. 3, we plot $h_d^*(t)$ at $t=0.05$ as a function of ε_F. As $\varepsilon_F\to-6$, the angle dependence of $h_d^*(t)$ vanishes and it converges to the value for the spherical Fermi surface. As ε_F is increased from −6, cubic distortion is gradually introduced to the Fermi surface as shown in Fig. 1, and $h_d^*(t)$ gradually develops anisotropy as a consequence. For $-6<\varepsilon_F\lesssim-2.5$, curves of $h_{[100]}^*(t)$ fall below that for the spherical Fermi surface, whereas $h_{[110]}^*(t)$ and $h_{[111]}^*(t)$ are enhanced over it. As ε_F approaches to −2, $h_d^*(t)$ is enhanced significantly irrespective of the field direction. Indeed, $h_d^*(t)$ for every field direction shows a singularity at $\varepsilon_F=-2$ where the Fermi surface touches the Brillouin zone at $\mathbf{k}_X$ with vanishing Fermi velocity $\mathbf{v}_F$ at these points. As a result, the contribution around these points becomes important in the integration $\langle K_{NN'}\rangle$ over the Fermi surface at low temperatures. This is the origin of the enhancement of $h_d^*(t)$ around $\varepsilon_F=-2$. For $\varepsilon_F>-2$, the difference between $h_{[110]}^*$ and $h_{[111]}^*$ is larger than that for $\varepsilon_F\lesssim-2.5$. This may be attributed to the topological difference of the Fermi surface. At $\varepsilon_F=0$, the tight-binding band is half filled and the Fermi-surface nesting occurs. However, $h_d^*(t)$ does not show any singularity around this energy.

Finally, we present results on the higher Landau-level contributions to the pair potential $\Delta(\mathbf{r})$, which is expanded as Eq. (27a). In general, when the system has n-fold symmetry around the field direction, mixing of higher Landau levels with multiples of n develops as the temperature is lowered.[70] Figure 4 shows the ratio Δ_N/Δ_0 as a function of T/T_c for $\varepsilon_F=-3$ (solid lines) and $\varepsilon_F=-2.02$ (dotted lines) with (a) $\mathbf{H}\|[100]$ ($N=4,8$ from bottom to top lines), (b) $\mathbf{H}\|[110]$ ($N=2,46$ from bottom to top lines), and (c) $\mathbf{H}\|[111]$ ($N=6$). One can clearly observe a general tendency that the mixing is more pronounced as the symmetry around $\mathbf{H}$ becomes lower as well as ε_F approaches closer to −2. Espe-

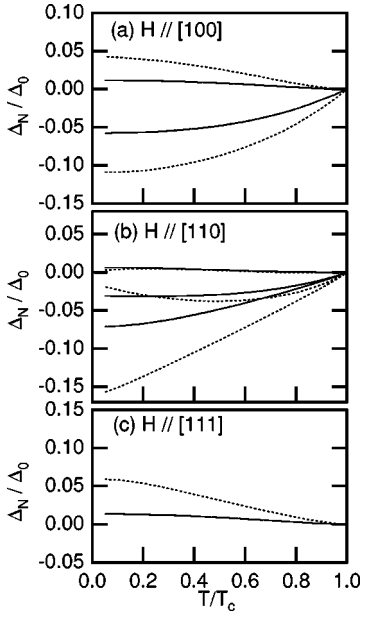

FIG. 4. The ratio Δ_N/Δ_0 of the expansion coefficients in Eq. (27a) as a function of temperature with (a) $\mathbf{H}\|[100]$, (b) $\mathbf{H}\|[110]$, and (c) $\mathbf{H}\|[111]$. The solid and dotted lines correspond to $\varepsilon_F=-3$ and $\varepsilon_F=-2.02$, respectively, with (a) $N=4,8$ from bottom to top (b) $N=2,4,6$ from bottom to top, and (c) $N=6$.

cially when $\mathbf{H}\|[110]$ and $\varepsilon_F=-2.02$, the $N=2$ contribution reaches up to nearly 15% of the lowest Landau-level contribution as $T\to 0$. The results suggest that the lowest-Landau-level approximation for the pair potential[9] is not quantitatively reliable at low temperatures for the field along low-symmetry directions, for complicated Fermi surfaces with divergences in the components of $\mathbf{v}_F$ perpendicular to $\mathbf{H}$, or for low-symmetry crystals.

V. SUMMARY

We have derived an efficient H_{c2} equation incorporating Fermi-surface anisotropy, gap anisotropy, and impurity scattering simultaneously. Basic results of Sec. II are summarized in Table I. This H_{c2} equation is a direct extension of the Rieck-Scharnberg equation[30] and reduces to the latter either (i) for the isotropic gap with arbitrary impurity scattering or (ii) in the clean limit with an arbitrary gap structure, as shown around Eq. (42). The operators introduced in Eq. (16) have been helpful to make the derivation simpler than that by Rieck and Scharnberg[30] and Rieck *et al.*.[31] The present method will be more suitable for extending the consideration to multicomponent order-parameter systems or to fields below H_{c2}.

We have also obtained a couple of analytic expressions near T_c (i) for H_{c2} up to the second order in $1-T/T_c$ and (ii) for the pair potential up to the first order in $1-T/T_c$. The latter result is given by Eq. (A8) with Eqs. (A9b) and (A4). They are useful to estimate the initial curvature of H_{c2} as well as the mixing of higher Landau levels in the pair potential.

The H_{c2} equation of Sec. II has also been extended in Sec. III to include p-wave impurity scattering, spin-orbit impurity scattering, and strong electron-phonon interactions.

Finally, we have presented numerical examples in Sec. IV performed for model Fermi surfaces from the three-dimensional tight-binding model. The results clearly demonstrate crucial importance of including detailed Fermi-surface structures in the calculation of H_{c2}. It has been found that, as the Fermi surface approaches the Brillouin zone boundary, the reduced critical field $h^*(t)$ in Eq. (1) is much enhanced over the value for the isotropic model with a significant upward curvature near T_c.

It is very interesting to see to what degree the upper critical field of classic type-II superconductors can be described quantitatively by calculations using realistic Fermi surfaces. The result by Butler[22,23] on high-purity Niobium provides promise to this issue. We have performed detailed evaluations of H_{c2} for various materials based on Eq. (35) by using Fermi surfaces from density-functional electronic-structure calculations as an input. The results are reported elsewhere.[75]

ACKNOWLEDGMENT

This research is supported by a Grant-in-Aid for Scientific Research from the Ministry of Education, Culture, Sports, Science, and Technology of Japan.

APPENDIX A: DETERMINATION OF (c_1,c_2) AND ANALYTIC EXPRESSION OF H_{c2} NEAR T_c

We here fix the constants (c_1,c_2) in Eqs. (16)–(18) conveniently so that H_{c2} near T_c can be described in terms of the lowest Landau level only. We also derive analytic expressions for B_1 and B_2 in Eq. (22) so that one can calculate them once the relevant Fermi-surface structure is given.

In the region $T\lesssim T_c$ where $l_c\to\infty$ in Eq. (14), we can perform a perturbation expansion with respect to the gradient operator $\mathbf{v}_F\cdot\boldsymbol{\partial}$. The equation for the νth-order solution $f_\nu^{(1)}$ $(\nu=0,1,\cdots)$ is obtained from Eq. (12a) as

$$f_\nu^{(1)}=\delta_{\nu 0}\frac{\phi\Delta}{\tilde{\varepsilon}_n'}+\frac{\hbar\langle f_\nu^{(1)}\rangle}{2\tau\tilde{\varepsilon}_n'}-\frac{\mathrm{sgn}(\varepsilon_n)}{2\tilde{\varepsilon}_n'}\hbar\mathbf{v}_F\cdot\boldsymbol{\partial}f_{\nu-1}^{(1)},\qquad \text{(A1)}$$

with $f_{-1}^{(1)}=0$. Noting $\phi(-\mathbf{k}_F)=\phi(\mathbf{k}_F)$, we solve Eq. (A1) self-consistently for $\langle f_\nu^{(1)}\rangle$, put the resulting expression back into Eq. (A1) to express $f_\nu^{(1)}$ explicitly, and finally take the Fermi-surface average $\langle\phi f_\nu^{(1)}\rangle$. This procedure yields

$$\langle\phi f_0^{(1)}\rangle=\frac{1}{\tilde{\varepsilon}_n'}\left(\langle\phi^2\rangle+\frac{\hbar\langle\phi\rangle^2}{2\tau|\varepsilon_n|'}\right)\Delta,\qquad \text{(A2a)}$$

$$\langle\phi f_2^{(1)}\rangle=\frac{1}{4\tilde{\varepsilon}_n'^3}\left\langle\left(\phi+\frac{\hbar\langle\phi\rangle}{2\tau|\varepsilon_n|'}\right)^2(\hbar\mathbf{v}_F\cdot\boldsymbol{\partial})^2\right\rangle\Delta,\qquad \text{(A2b)}$$

$$\langle \phi f_4^{(1)} \rangle = \frac{1}{16\tilde{\varepsilon}_n'^5}\left[\left\langle\left(\phi + \frac{\hbar\langle\phi\rangle}{2\tau|\varepsilon_n|'}\right)^2(\hbar\mathbf{v}_F\cdot\boldsymbol{\partial})^4\right\rangle + \frac{\hbar}{2\tau|\varepsilon_n|'}\left\langle\left(\phi + \frac{\hbar\langle\phi\rangle}{2\tau|\varepsilon_n|'}\right)(\hbar\mathbf{v}_F\cdot\partial)^2\right\rangle^2\right]\Delta, \tag{A2c}$$

with $|\varepsilon_n|' \equiv |\varepsilon_n| - i\mu_B B\,\mathrm{sgn}(\varepsilon_n)$, and $\langle\phi f_1^{(1)}\rangle = \langle\phi f_3^{(1)}\rangle = 0$.

Let us substitute Eq. (A2) into Eq. (12b), replace the gradient operator by the right-hand side of Eq. (14), put $B = B_{c2}$ in l_c of Eq. (15), and expand $|\varepsilon_n|'$ with respect to $\mu_B B_{c2}/|\varepsilon_n|$. We thereby obtain the self-consistency equation near T_c as

$$\begin{aligned} &w_{0,0}\Delta + \frac{B_{c2}}{B_1}[w_{2,2}a^\dagger a^\dagger + w_{2,2}^* aa - w_{2,0}(aa^\dagger + a^\dagger a)]\Delta \\ &+ \left(\frac{B_{c2}}{B_1}\right)^2[w_{4,4}a^\dagger a^\dagger a^\dagger a^\dagger + w_{4,4}^* aaaa \\ &- w_{4,2}(aa^\dagger a^\dagger a^\dagger + a^\dagger aa^\dagger a^\dagger + a^\dagger a^\dagger aa^\dagger + a^\dagger a^\dagger a^\dagger a) \\ &- w_{4,2}^*(a^\dagger aaa + aa^\dagger aa + aaa^\dagger a + aaaa^\dagger) \\ &+ w_{4,0a}(aa^\dagger aa^\dagger + a^\dagger aaa^\dagger + aa^\dagger a^\dagger a + a^\dagger aa^\dagger a) \\ &+ w_{4,0b}(aaa^\dagger a^\dagger + a^\dagger a^\dagger aa) + w_P]\Delta = 0. \end{aligned} \tag{A3}$$

Here B_1 is given in Eq. (22), which is incorporated into the denominator for convenience. The functions $w_{\nu,\mu} = w_{\nu,\mu}(T)$ and $w_P = w_P(T)$ are dimensionless and defined by

$$w_{0,0}(T) \equiv \ln\frac{T_{c0}}{T} - (1-\langle\phi\rangle^2)2\pi T\sum_{n=0}^{\infty}\left(\frac{1}{\varepsilon_n} - \frac{1}{\tilde{\varepsilon}_n}\right), \tag{A4a}$$

$$w_{2,2}(T) \equiv \frac{B_1\hbar^2\pi^2 T}{2\Phi_0}\sum_{n=0}^{\infty}\frac{1}{\tilde{\varepsilon}_n^3}\left\langle\left(\phi + \frac{\hbar\langle\phi\rangle}{2\tau\varepsilon_n}\right)^2\overline{v}_{F+}^2\right\rangle, \tag{A4b}$$

$$w_{2,0}(T) \equiv \frac{B_1\hbar^2\pi^2 T}{2\Phi_0}\sum_{n=0}^{\infty}\frac{1}{\tilde{\varepsilon}_n^3}\left\langle\left(\phi + \frac{\hbar\langle\phi\rangle}{2\tau\varepsilon_n}\right)^2|\overline{v}_{F+}|^2\right\rangle, \tag{A4c}$$

$$w_{4,4}(T) \equiv \frac{B_1^2\hbar^4\pi^3 T}{8\Phi_0^2}\sum_{n=0}^{\infty}\frac{1}{\tilde{\varepsilon}_n^5}\left[\left\langle\left(\phi + \frac{\hbar\langle\phi\rangle}{2\tau\varepsilon_n}\right)^2\overline{v}_{F+}^4\right\rangle + \frac{\hbar}{2\tau\varepsilon_n}\left\langle\left(\phi + \frac{\hbar\langle\phi\rangle}{2\tau\varepsilon_n}\right)\overline{v}_{F+}^2\right\rangle^2\right], \tag{A4d}$$

$$w_{4,2}(T) \equiv \frac{B_1^2\hbar^4\pi^3 T}{8\Phi_0^2}\sum_{n=0}^{\infty}\frac{1}{\tilde{\varepsilon}_n^5}\left[\left\langle\left(\phi + \frac{\hbar\langle\phi\rangle}{2\tau\varepsilon_n}\right)^2\overline{v}_{F+}^2|\overline{v}_{F+}^2|\right\rangle + \frac{\hbar}{2\tau\varepsilon_n}\left\langle\left(\phi + \frac{\hbar\langle\phi\rangle}{2\tau\varepsilon_n}\right)\overline{v}_{F+}^2\right\rangle\left\langle\left(\phi + \frac{\hbar\langle\phi\rangle}{2\tau\varepsilon_n}\right)|\overline{v}_{F+}|^2\right\rangle\right], \tag{A4e}$$

$$w_{4,0a}(T) \equiv \frac{B_1^2\hbar^4\pi^3 T}{8\Phi_0^2}\sum_{n=0}^{\infty}\frac{1}{\tilde{\varepsilon}_n^5}\left[\left\langle\left(\phi + \frac{\hbar\langle\phi\rangle}{2\tau\varepsilon_n}\right)^2|\overline{v}_{F+}|^4\right\rangle + \frac{\hbar}{2\tau\varepsilon_n}\left\langle\left(\phi + \frac{\hbar\langle\phi\rangle}{2\tau\varepsilon_n}\right)|\overline{v}_{F+}|^2\right\rangle^2\right], \tag{A4f}$$

$$w_{4,0b}(T) \equiv \frac{B_1^2\hbar^4\pi^3 T}{8\Phi_0^2}\sum_{n=0}^{\infty}\frac{1}{\tilde{\varepsilon}_n^5}\left[\left\langle\left(\phi + \frac{\hbar\langle\phi\rangle}{2\tau\varepsilon_n}\right)^2|\overline{v}_{F+}|^4\right\rangle + \frac{\hbar}{2\tau\varepsilon_n}\left|\left\langle\left(\phi + \frac{\hbar\langle\phi\rangle}{2\tau\varepsilon_n}\right)\overline{v}_{F+}^2\right\rangle\right|^2\right], \tag{A4g}$$

$$w_P(T) \equiv -(\mu_B B_1)^2 2\pi T\sum_{n=0}^{\infty}\left[\frac{\langle\phi\rangle^2}{\varepsilon_n^3} + \frac{1-\langle\phi\rangle^2}{\tilde{\varepsilon}_n^3}\right]. \tag{A4h}$$

We next substitute Eq. (22) into Eq. (A3) and expand $w_{\nu,\mu}$ in Eq. (A3) up to the $(4_{-1}/2)$th order in $1-t$. We also put $w_P(T) = w_P(T_c)$. This procedure yields three equations corresponding to order 1, $1-t$, and $(1-t)^2$. The equation of order 1 is given by $w_{0,0}(T_c)\Delta = 0$. It determines T_c at $H = 0$ by

$$\ln\frac{T_{c0}}{T_c} = (1-\langle\phi\rangle^2)\left[\psi\left(\frac{1}{2} + \frac{\hbar}{4\pi\tau T_c}\right) - \psi\left(\frac{1}{2}\right)\right], \tag{A5}$$

with $\psi(x)$ the digamma function.

The equation of order $1-t$ in Eq. (A3) is obtained as

$$\begin{aligned} &[-T_c w_{0,0}'(T_c) - w_{2,0}(T_c)(2a^\dagger a + 1) + w_{2,2}(T_c)a^\dagger a^\dagger \\ &+ w_{2,2}^*(T_c)aa]\Delta(\mathbf{r}) = 0. \end{aligned} \tag{A6}$$

To solve it, we use the arbitrariness in (c_1, c_2) and impose $w_{2,2}(T_c) = 0$. Noting Eqs. (A4b) and (18), this condition is transformed into a dimensionless form as

$$\chi_{xx}c_2^2 + 2i\chi_{xy}c_1c_2 - \chi_{yy}c_1^2 = 0, \tag{A7}$$

where $\chi_{ij} = \chi_{ij}(T_c)$ is defined by Eq. (20). Equation (A7) can be solved easily in terms of c_2. Substituting the resulting expression into Eq. (17) and choosing c_1 real, we obtain Eq. (19).

Now that $w_{2,2}(T_c) = 0$ in Eq. (A6), the highest field for a nontrivial solution corresponds to the lowest Landau level where $w_{2,0}(T_c) = -T_c w_{0,0}'(T_c)$. Introducing $R \equiv -T_c w_{0,0}'(T_c)$, which is given explicitly as Eq. (24), and using Eqs. (A4a), (A4c), (18), and (19), we obtain the expression for B_1 as Eq. (23).

We finally consider the equation of order $(1-t)^2$ in Eq. (A3) and expand the pair potential as

$$\Delta(\mathbf{r}) = \Delta_0\{\psi_{0\mathbf{q}}(\mathbf{r}) + (1-t)[r_2\psi_{2\mathbf{q}}(\mathbf{r}) + r_4\psi_{4\mathbf{q}}(\mathbf{r})]\}, \tag{A8}$$

where $\psi_{N\mathbf{q}}(\mathbf{r})$ is defined by Eq. (21), and (Δ_0, r_2, r_4) are the expansion coefficients with (r_2, r_4) describing relative mixing of higher Landau levels in the pair potential. Let us substitute Eq. (A8) into Eq. (A3), multiply the equation of order $(1-t)^2$ by $\psi_{N\mathbf{q}}^*(\mathbf{r})$, and perform integration over $\mathbf{r}$. The resulting equations for $N = 0, 2, 4$ yield

$$B_2 = \frac{\frac{1}{2}T_c^2 w_{0,0}^{(2)} + T_c w_{2,0} + w_{4,0a} + 2w_{4,0b} + w_{\mathrm{P}}}{R} B_1, \tag{A9a}$$

$$r_2 = -\frac{T_c w'_{2,2} + 6w_{4,2}}{2\sqrt{2}R}, \quad r_4 = \frac{\sqrt{6}w_{4,4}}{4R}, \tag{A9b}$$

respectively. The functions in Eqs. (A9a) and (A9b) are defined by Eqs. (A4) and (24) and should be evaluated at T_c. In the clean limit $\tau \to \infty$, these functions acquire simple expressions as

$$R = T_c^2 w_{0,0}^{(2)} = 1, \quad T_c w'_{2,0} = -2, \quad T_c w'_{2,2} = 0, \tag{A10a}$$

$$w_{4,\mu} = \frac{31\zeta(5)}{[7\zeta(3)]^2} \frac{\langle \phi^2 |\overline{v}_{\mathrm{F}+}|^{4-\mu} \overline{v}_{\mathrm{F}+}^{\mu} \rangle}{\langle \phi^2 |\overline{v}_{\mathrm{F}+}|^2 \rangle^2}, \tag{A10b}$$

$$w_{\mathrm{P}} = -\frac{7\zeta(3)(\mu_{\mathrm{B}} B_1)^2}{4(\pi T_c)^2}, \tag{A10c}$$

with $\mu = 0, 2, 4$ and $w_{4,0} \equiv w_{4,0a} = w_{4,0b}$. Equation (A9) with Eq. (A10), includes the result by Hohenberg and Werthamer[9] for cubic materials and also the one by Takanaka[18] for uniaxial materials in the relevant order, both except the Pauli term w_{P}. Thus, we have extended the results by Hohenberg and Werthamer[9] and Takanaka[18] to arbitrary crystal structures and impurity-scattering time, including also Pauli paramagnetism.

Equation (A9) reveals a close connection of both the curvature in $H_{c2}(T \lesssim T_c)$ and the mixing of higher Landau levels in $\Delta(\mathbf{r})$ with the Fermi-surface structure. For example, we realize from Eq. (A9b) with Eqs. (A10), (18), and (26) that the mixing of $N=2$ Landau level is absent for cubic materials where $c_1 = c_2 = 1$. This is not the case for low-symmetry crystals, however. Equation (A9) enables us to estimate the curvature and the mixing based on Fermi-surface structures from detailed electronic-structure calculations.

APPENDIX B: PROOF OF EQ. (41)

The first expression in Eq. (41a) can be proved by induction as follows. First of all, $\eta_0 = R_0$ is transformed from Eq. (37a) as[76]

$$\begin{aligned}
\eta_0 &= \frac{1}{1 + \dfrac{x^2}{1 + \dfrac{2x^2}{1 + \cdots}}} = \frac{\sqrt{2}}{x} \mathrm{e}^{1/2x^2} \int_{1/\sqrt{2}x}^{\infty} \mathrm{e}^{-s^2} ds \\
&= \int_0^{\infty} \exp\left(-s - \frac{x^2}{2} s^2 \right) ds = \frac{2}{\sqrt{\pi}} \int_0^{\infty} \frac{\mathrm{e}^{-s^2}}{1 + 2x^2 s^2} ds \\
&= \int_0^{\infty} \frac{2s\mathrm{e}^{-s^2}}{\sqrt{1 + 2x^2 s^2}} ds.
\end{aligned} \tag{B1}$$

Thus, Eq. (41a) holds for $N=0$. The last expression in Eq. (B1) is the same integral which appears in Eq. (26) of Hohenberg and Werthamer.[9] We next rewrite Eq. (37a) with respect to η_N in Eq. (40a) as

$$\eta_N = \begin{cases} (-\eta_0 + 1)/x^2 & (N = 1) \\ (-\eta_{N-1} + \sqrt{N-1}\,\eta_{N-2})/\sqrt{N}x^2 & (N \geqslant 2) \end{cases}. \tag{B2}$$

Using Eqs. (B1) and (B2), it is easy to see that Eq. (41a) holds for $N=1$. Proceeding to the general case, we assume that Eq. (41a) is valid for $N \leqslant M-1$. We also remember the following properties of the Hermite polynomials:

$$H_N(s) - 2sH_{N-1}(s) + 2(N-1)H_{N-2}(s) = 0, \tag{B3a}$$

$$\int_0^{\infty} s^k H_N(s) \mathrm{e}^{-s^2} ds = 0 \quad (k \leqslant N-1). \tag{B3b}$$

Then η_M is obtained explicitly by using Eq. (B2) as

$$\begin{aligned}
\eta_M &= \frac{1}{\sqrt{M}x^2}[-\eta_{M-1} + \sqrt{M-1}\,\eta_{M-2}] \\
&= \int_0^{\infty} \frac{2s^{M-2}[-sH_{M-1}(s) + (M-1)H_{M-2}(s)]\mathrm{e}^{-s^2}}{\sqrt{\pi M!}x^2(1 + 2x^2 s^2)} ds \\
&= \int_0^{\infty} \frac{-s^{M-2}H_M(s)\mathrm{e}^{-s^2}}{\sqrt{\pi M!}x^2(1 + 2x^2 s^2)} ds \\
&= \int_0^{\infty} \frac{s^{M-2}H_M(s)\mathrm{e}^{-s^2}}{\sqrt{\pi M!}x^2} \left(1 - \frac{1}{1 + 2x^2 s^2} \right) ds \\
&= \frac{2}{\sqrt{\pi M!}} \int_0^{\infty} \frac{s^M H_M(s)\mathrm{e}^{-s^2}}{1 + 2x^2 s^2} ds.
\end{aligned} \tag{B4}$$

Thus, we have established the first expression in Eq. (41a). The proof for the second expression proceeds in the same way by using partial integrations for η_0 and η_{N-2} in Eq. (B2). Equation Eq. (41b) can be proved similarly by induction, starting from $R_1 = 1$ and using Eq. (37b).

[1] A. A. Abrikosov, Zh. Eksp. Teor. Fiz. **32**, 1442 (1957) [Sov. Phys. JETP **5**, 1174 (1957)].
[2] V. L. Ginzburg and L. D. Landau, Zh. Eksp. Teor. Fiz. **20**, 1064 (1950).
[3] L. P. Gor'kov, Zh. Eksp. Teor. Fiz. **37**, 833 (1959); Sov. Phys. JETP **10**, 593 (1960).
[4] K. Maki, Physics (Long Island City, N.Y.) **1**, 21 (1964).
[5] P. G. de Gennes, J. Phys.: Condens. Matter **3**, 79 (1964).
[6] E. Helfand and N. R. Werthamer, Phys. Rev. Lett. **13**, 686 (1964); Phys. Rev. **147**, 288 (1966).
[7] N. R. Werthamer, E. Helfand, and P. C. Hohenberg, Phys. Rev. **147**, 295 (1966).
[8] K. Maki, Phys. Rev. **148**, 362 (1966).
[9] P. C. Hohenberg and N. R. Werthamer, Phys. Rev. **153**, 493 (1967).
[10] G. Eilenberger, Phys. Rev. **153**, 584 (1967).
[11] G. Eilenberger and V. Ambegaokar, Phys. Rev. **158**, 332 (1967).
[12] N. R. Werthamer and W. L. McMillan, Phys. Rev. **158**, 415 (1967).
[13] L. W. Gruenberg and L. Gunther, Phys. Rev. **176**, 606 (1968).
[14] L. F. Mattheiss, Phys. Rev. B **1**, 373 (1970).
[15] K. Takanaka and T. Nagashima, Prog. Theor. Phys. **43**, 18 (1970).
[16] K. Takanaka, Prog. Theor. Phys. **46**, 357 (1971).
[17] D. Rainer and G. Bergmann, J. Low Temp. Phys. **14**, 501 (1974).
[18] K. Takanaka, Phys. Status Solidi B **68**, 623 (1975).
[19] H. Teichler, Phys. Status Solidi B **69**, 501 (1975).
[20] H.-W. Pohl and H. Teichler, Phys. Status Solidi B **75**, 205 (1976).
[21] P. Entel and M. Peter, J. Low Temp. Phys. **22**, 613 (1976).
[22] W. H. Butler, in *Superconductivity in d- and f-Band Metals*, edited by H. Suhl and M. B. Maple (Academic, New York, 1980) p. 443.
[23] W. H. Butler, Phys. Rev. Lett. **44**, 1516 (1980).
[24] D. W. Youngner and R. A. Klemm, Phys. Rev. B **21**, 3890 (1980).
[25] K. Scharnberg and R. A. Klemm, Phys. Rev. B **22**, 5233 (1980).
[26] M. Schossmann and E. Schachinger, Phys. Rev. B **30**, 1349 (1984).
[27] M. Schossmann and E. Schachinger, Phys. Rev. B **33**, 6123 (1986).
[28] M. Prohammer and E. Schachinger, Phys. Rev. B **36**, 8353 (1987).
[29] M. Prohammer and J. P. Carbotte, Phys. Rev. B **42**, 2032 (1990).
[30] C. T. Rieck and K. Scharnberg, Physica B **163**, 670 (1990).
[31] C. T. Rieck, K. Scharnberg, and N. Schopohl, J. Low Temp. Phys. **84**, 381 (1991).
[32] Z. Tešanović, M. Rasolt, and L. Xing, Phys. Rev. B **43**, 288 (1991).
[33] E. Langmann, Phys. Rev. B **46**, 9104 (1992).
[34] W. Pitscheneder and E. Schachinger, Phys. Rev. B **47**, 3300 (1993).
[35] M. R. Norman, A. H. MacDonald, and H. Akera, Phys. Rev. B **51**, 5927 (1995).
[36] T. Kita, J. Photogr. Sci. **67**, 2075 (1998).
[37] T. Maniv, V. Zhuravlev, I. Vagner, and P. Wyder, Rev. Mod. Phys. **73**, 867 (2001).
[38] K. Yasui and T. Kita, Phys. Rev. B **66**, 184516 (2002).
[39] P. Miranović, K. Machida, and V. G. Kogan, J. Phys. Soc. Jpn. **72**, 221 (2003).
[40] T. Dahm and N. Schopohl, Phys. Rev. Lett. **91**, 017001 (2003).
[41] T. Kita, Phys. Rev. B **68**, 184503 (2003).
[42] See, e.g., W. Kohn, Rev. Mod. Phys. **71**, 1253 (1999); R. O. Jones and O. Gunnarsson, *ibid.* **61**, 689 (1989).
[43] See, e.g., G. Blatter, M. V. Feigel'man, V. B. Geshkenbein, A. I. Larkin, and V. M. Vinokur, Rev. Mod. Phys. **66**, 1125 (1994).
[44] J. Bardeen, L. N. Cooper, and J. R. Schrieffer, Phys. Rev. **108**, 1175 (1957).
[45] See, *Superconductivity*, edited by R. D. Parks (Marcel Dekker, New York, 1969).
[46] D. R. Tilley, G. J. van Gurp, and C. W. Berghout, Phys. Lett. **12**, 305 (1964).
[47] T. McConville and B. Serin, Phys. Rev. **140**, A1169 (1965).
[48] D. K. Finnemore, T. F. Stromberg, and C. A. Swenson, Phys. Rev. **149**, 231 (1966).
[49] R. Radebaugh and P. H. Keesom, Phys. Rev. **149**, 217 (1966).
[50] S. J. Williamson, Phys. Rev. B **2**, 3545 (1970).
[51] F. M. Sauerzopf, E. Moser, H. W. Weber, and F. A. Schmidt, J. Low Temp. Phys. **66**, 191 (1987).
[52] For early accomplishments on anisotropic effects, see, *Anisotropic Effects in Superconductors*, edited by H. W. Weber (Plenum, New York, 1977).
[53] H. R. Kerchner, D. K. Christen, and S. T. Sekula, Phys. Rev. B **21**, 86 (1980).
[54] H. W. Weber, E. Seidl, C. Laa, E. Schachinger, M. Prohammer, A. Junod, and D. Eckert, Phys. Rev. B **44**, 7585 (1991).
[55] Y. Muto, N. Yokota, K. Nato, and A. Hoshi, Phys. Lett. **45A**, 99 (1973).
[56] J. A. Woollam, R. B. Somoano, and P. O'Connor, Phys. Rev. Lett. **32**, 712 (1974).
[57] B. J. Dalrymple and D. E. Prober, J. Low Temp. Phys. **56**, 545 (1984).
[58] P. B. Allen, Phys. Rev. B **13**, 1416 (1976).
[59] We here consider $V(\mathbf{k}_F,\mathbf{k}'_F)$ calculated just above T_c. Thus, our $V(\mathbf{k}_F,\mathbf{k}'_F)$ does not contain any feedback effects below T_c which may lower its symmetry from the normal state. For the feedback effects in superfluid ^{3}He, see e.g., A. J. Leggett, Rev. Mod. Phys. **47**, 331 (1975).
[60] V. L. Pokrovskii, Zh. Eksp. Teor. Fiz. **40**, 641 (1961); [Sov. Phys. JETP **13**, 447 (1961)].
[61] G. M. Eliashberg, Zh. Eksp. Teor. Fiz. **38**, 966 (1960); [Sov. Phys. JETP **11**, 696 (1960)].
[62] For a review on the topic and notations, see P. B. Allen, and B. Mitrović, in *Solid State Physics* 37, edited by H. Ehrenreich, F. Seitz, and D. Turnbull (Academic, New York, 1982) p. 62.
[63] H. J. Choi, D. Roundy, H. Sun, M. L. Cohen, and S. G. Louie, Phys. Rev. B **66**, 020513 (2002); Nature (London) **418**, 758 (2002).
[64] G. Eilenberger, Z. Phys. **214**, 195 (1968).
[65] A. I. Larkin and Y. N. Ovchinnikov, Zh. Eksp. Teor. Fiz. **55**, 2262 (1968) [Sov. Phys. JETP **28**, 1200 (1969)].
[66] For a review on the quasiclassical theory, see e.g., J. W. Serene and D. Rainer, Phys. Rep. **101**, 221 (1983).
[67] See, e.g., A. E. Koshelev, Phys. Rev. Lett. **83**, 187 (1999), and references therein.
[68] T. Kita, Phys. Rev. B **69**, 144507 (2004).
[69] L. P. Gor'kov, Zh. Eksp. Teor. Fiz. **37**, 1407 (1959); [Sov. Phys. JETP **10**, 998 (1960)].
[70] T. Kita, J. Photogr. Sci. **67**, 2067 (1998).
[71] More exactly, the coefficient c_2 determined by Eqs. (17) and (A7) is chosen as real in the basis functions used by Rieck and Scharnberg.[30]

[72] It should be noted that β is not independent of ε_n but depends on the sign of ε_n. Thus Eq. (32) may be somewhat misleading, but it allows us a compact notation as seen from Eq. (29).
[73] See, e.g., *Handbook of Mathematical Functions with Formulas, Graphs, and Mathematical Tables*, edited by M. Abramowitz and I. A. Stegun (Wiley, New York, 1972).
[74] H. Teichler, Philos. Mag. **69**, 775 (1975).
[75] M. Arai and T. Kita, cond-mat/0404628 (unpublished).
[76] H. S. Wall, *Analytic Theory of Continued Fractions* (AMS Chelsea Publishing, Rhode Island, 2000) p. 358.